Detection of foodborne pathogens using microfluidic channels

Xingkai Hao

A thesis submitted to the
Faculty of Graduate and Postdoctoral Studies
in partial fulfillment of the requirements for the
M.A.Sc degree in Chemical Engineering

Chemical Engineering Department
Faculty of Engineering
University of Ottawa

© Xingkai Hao, Ottawa, Canada, 2015

Abstract

Rapid detection of foodborne pathogen is one of the most urgent problems in the world, because foodborne pathogen could cause serious illness, such as nausea, vomiting and diarrhea. We have developed a sensitive microfluidic system based on dendrimers and aptamers for rapid detection of Escherichia coli O157:H7 at very low cells concentration. Dendrimers, with high level of functional groups and homogeneous spherical shape, are prefect nanoscale polymers used as a template material by increasing sensitivity and specificity of analytes detection in microfluidics. In this work, we develop a sensitive microfluidic system based on dendrimers and aptamers for detecting Escherichia coli O157:H7 at very low cell concentrations. Carboxyl functionalized G7-polyamidoamine (PAMAM-COOH) dendrimers are immobilized on (3-aminopropyl)-trimethoxysilane (APTMS) pretreated microfluidic channels. The aptamers are subsequently conjugated on the immobilized dendrimes through chemicals. The sensitivity and specificity are validated by injecting fluorescein isothiocyanate (FITC) labelled *Escherichia coli O157:H7* at various cells concentration into the resulting microchannels, indicating that the detectable cells concentration can be reached as low as 10^2 (cells/ml) and the detection time is 10 hours. To further exploit and improve the work efficiency our microfluidic device, the microfluidic channel is designed into a staggered herringbone microchannel (SHM) to create the chaotic dynamics inside the microfluidic device, and the SHM is then simulated by a COMSOL software showing

that the staggered herringbone structures can improve chaotic dynamics of designed microchannel and will enhance the probability of particles to attach on the surface of microdevice. All the results show that our approach has the potential to develop the field of rapid and accurate detection on foodborne pathogens.

Résumée

Le dendrimère, avec un niveau élevé de groupes fonctionnels et la forme sphériquement homogène, est un très bon polymère namométriques utilisé comme matériau modèle pour augmenter la sensibilité et la spécificité de la détection des analytes dans microfluidique. Dans ce travail, nous développons un système microfluidique sensible basé sur des dendrimères et des aptamères pour détecter Escherichia coli O157:H7 des concentrations très faibles de cellules. Fonctionnalité par carboxyle, G7- polyamidoamine (PAMAM-COOH) dendrimères sont immobilisés sur des canaux microfluidiques prétraités par (3-aminopropyl)-trimethoxysilane (APTMS). Les aptamères sont ensuite conjugués sur les dendrimes immbilisé à travers des produits chimiques. La sensibilité et la spécificité sont validés en injectant Escherichia coli O157:H7, marqué de FITC et à différentes concentration de cellules, dans les microcanaux de résultat. Cela indique que la concentration des cellules détectables peut atteindre le plus bas 10^2 (cellules/ml) et le temps de détection est quelques heures . Pour exploiter davantage et améliorer l'efficacité du travail de notre dispositif microfluidique , le canal microfluidique est conçu comme un microcanal de chevrons en quinconce (SHM) pour créer le chaos dynamique à l'intérieur du dispositif microfluidique, et la SHM est ensuite simulé par un logiciel de COMSOL qui montre que la SHM structures peuve améliorer le chaos dynamique dans les microcanaux conçu et permettre d'améliorer la probabilité de particules pour attacher sur la surface du microdispositif . Tous les résultats montrent que notre approche a la potentialiité de développer le domaine de la détection rapide et

précise sur les pathogènes alimentaires.

Acknowledgements

First and foremost, I would like to show my deepest gratitude to my supervisor, Dr. Xudong Cao, a respectable, responsible and resourceful scholar, who has provided me with valuable guidance in every stage of experiment doing and thesis writing. Without his enlightening instruction, impressive kindness and patience, I could not have completed my thesis. His keen and vigorous academic observation enlightens me not only in this thesis but also in my future study.

To Dr. Min for the help of discussion about my thesis and the supplement of *Escherichia coli O157:H7*. His suggestions give me great inspiration about my academic.

I shall extend my thanks to Mr. Jacob Yep for all his kindness and help. I would also like to Mr. Louis Tremblay for the help of using and repairing of all the equipment. Next, I would thank all my teachers who have helped me to develop the fundamental and essential academic competence.

My sincere appreciation also goes to my colleagues Yubo Qin for all his pictures and support, and Yuqian Jiang as well as Zizhen Li for the help and the good moments together.

Lastly, I am extremely grateful to my father, mother and my wife for the constant love and encouragement.

Table of Content

Contents

List of Figure

List of Scheme

List of Table

Abbreviations

Abbreviations	Name
APTMS	3-aminopropyltrimethoxysilane
AFM	Atomic force microscopy
BSA	Bovine serum albumin
EDA	Ethylenediamine
CY3	Cyanine 3
ESI–MS	Electrospray–ionization mass spectroscopy
EPR	Electron paramagnetic resonance
FTIR	Fourier transform infrared spectroscopy
FITC	Fluorescein isothiocyanate
HUS	Haemolytic uraemic syndrome
HPLC	High-performance liquid chromatography
GUD	Glucuronidase
LOD	Limit of detection
MPTMS	3-mercaptopropyltrimethoxy silane
PAMAM	Polyamidoamine
PCR	Polymerase chain reaction
PDMS	Polydimethylsiloxane
PMSA	Prostate-specific membrane antigen
PPEGMA	Poly(poly(ethylene glycol)methacrylate)

PTFFS	Particle tracing for fluid flow simulation
QDs	Quantum dots
Re	Reynolds
SEC	Size-exclusion chromatography
SELEX	Exponential enrichment
SHMs	Staggered herringbone microchannels
TDSS	Transport of diluted species simulation
XPS	X-ray photoelectron spectroscopy

Chapter 1. Introduction

Rapid detection and identification of foodborne pathogens is in urgent need to protect the public health. Pathogenic bacteria problems are easiest to outbreak in food industry, and if researchers fail to discover certain pathogens, the result for the public health will be fatal [1-4]. A large number of researchers are devoting to inspect the foodborne pathogens. Recently, July 21, 2014, Canadian Food Inspection Agency (CFIA) has recalled several fruits nationally because they were contaminated by *Listeria*. [5] Among these pathogen detection methods studies, *Escherichia coli* is the most commonly used model pathogen and *Salmonellae* is the most favorable bacteria studied for rapid detection. As for other pathogenic bacteria which should be detected named *Legionella*, *Campylobacter*, and *Listeria*, respectively. [6]

New technologies have improved the detection methods in a large scale, but the public still need a cheaper, faster and more sensitive way to inspect pathogenic bacteria. The new trend should have following advantages. Firstly, the detection devices should be mass produced with cheaper price as well as a small size. Secondly, the devices should have abilities working with very small volumes of sample in microscale or less and also the chemical reagents will have a reasonable price. Thirdly, the detection time should be better limited to several hours and the devices should be easy for people to use. Fourthly, the devices should be able to detect several pathogens at the same time. Fifthly, the read out equipment should be portable and inexpensive. Finally, the devices should be able to detect very small

number of bacteria. Ideally the limit of detection (LOD) should be limited less 10 cells/ml.

In conventional detection methods, the most popular one is plate culture methods because it is the most sensitive and reliable method. [7-9] But, the disadvantages of the plate culture method are time-consuming and are complicated. Normally, the detection time of plate culture method is 5 days. [6] [10] Although many other rapid detection methods, such as polymerase chain reaction (PCR) [6], ELISIA [10-12], Electrophoresis [13, 14] and Flow cytometry [15, 16], have been developed to reduce the detection time, the final result readout format of these technologies are completed within minutes or hours, and these rapid detection techniques are still need time-consuming bacterial enrichment process to achieve a detectable bacterial concentration. Therefore, food inspection processes still require a long overall time. Bacterial enrichment is an inevitable process in food inspection, because numbers of foodborne pathogens in real-world foods samples are usually very low, and small dose of some foodborne pathogens could cause serious symptoms, for example, the infection dose of *E.coli* is 50 cell/ml and it could cause people getting nausea, vomiting and diarrhea. [17] Therefore, researchers use bacterial enrichment methods to increase population of the foodborne pathogens, and collect these expanded foodborne pathogens to a detectable level which is suitable for above mentioned existing technologies. [18] As a result, for the safety of public health, even though bacterial culture enrichment is time-consuming, it is still the gold standard as well as the bottle neck in food inspection. [18]

New methods, microfluidics, have been developed over the last 20 years in pathogen detection and researchers have successful detected pathogen in these micodevices [19-22], but these devices still cannot meet demands for rapid detection (i.e. low accuracy and require expensive machines). Usually, microfluidics depends on specificity of antibodies or DNAs and can be divided into three types relying on the working theory, optical [23], electrochemical [24] and piezoelectric [25]. For electrochemical and piezoelectric microfluidic systems are hard to control, expensive and unreliable, but it can detect very low concentration pathogens. [6] However, optical based microfluidics are easy to operate and directly, but they have a high LOD. To author's best knowledge, to take *E.coli* detection for example, the lowest LOD for optical based microfluidics is 10^3 cells/ml [21].

Recently, dendrimers are developed as a hopeful candidate for rapid diagnostic system. [26-29] Dendrimers can form homogeneous, dense, compacted and stable layers on substrate surfaces, and the multiple branch ends of dendrimers are available for successive conjugation reactions [30]. What is more, the capture surfaces of dendirmers are relatively larger than linear analogues leading to high capture probability [30]. Dendrimers have been greatly used in biosensors, and some groups coated glass surfaces with carboxyl terminated dendrimers, showing that the resulting surfaces can prevent protein nonspecific absorption and are also suitable for conjugation of antibodies. [31]

In this study, balancing the advantages and disadvantages of previous microfluidic systems and using the superiority of dendrimers, we will develop a

simple and fast method for pathogen detection by introducing two layers to modify the surface of PDMS based microfluidics. So, two materials will be conjugated on the surface of microchannels. The first layer material is dendrimers which can act as a non-fouling agent to prevent nonspecific absorption of the channel surface [32]. Therefore, when dendrimers are applied on the surface of microfluidics, dendrimers could decrease the background noise. Furthermore, dendrimers have multiple branch structures [30] which can bind more aptamers, consequently, detection sensitivity of microchannels is improved. The second layer is constituted by aptamers. The aptamers, providing specificity to *E.coli*, could one-one correspondence bind with these branch structures of dendrimers by chemical links, and because aptamers have better affinity, better stability and smaller molecular size than traditional antibodies. [33] As a result, chances for aptamers to attach with analysts will be much greater, so the detection sensitivity will be improved in a further step. Here, nonpathogenic fluorescence labelled Escherichia coli was injected into the objective microchannels for a 10 hours and the limit of detection was analyzed accordingly. What is more, in order to decrease the detection time and increase the microchannel work efficiency, the straight microchannel is redesigned into a grooved structure microchannel to enhance the opportunities of analytes attaching to these aptamers. The redesigned microchannel was then simulated by a Comsol software.

The final results shows that comparing with electrochemical and piezoelectric microfluidic systems, our microchannel applied in this project is relatively simple, as

the detection device is only a fluorescent microscope; moreover, the LOD in our approach is 10^2 cells/ml and the detection time is only 10 hours, which are dramatically lower and faster than other optical based microfluidics. [21, 22, 25, 34]

Chapter 2. Literature Survey

2.1 *Escherichia coli O157:H7* Infection in Humans

Escherichia coli O157:H7 is an enterohemorrhagic serotype of the bacterium Escherichia coli [35] and it could cause *abdominal cramps* and *acute hemorrhagic diarrhea* [36]. O157:H7 is named because that the *Escherichia coli* can express the 157th somatic (O) antigen identified and the 7th flagella(H) antigen. [2] In history, it was first extracted in 1982. At that time, 47 people got sick in Michigan and Oregon after eating *Escherichia coli O157:H7* contaminated hamburgers. [37] In 1983, Johnson found the reason of *Escherichia coli O157:H7* causing serious diseases was that the bacteria can produce a “shiga-like toxin” and could cause post-diarrhoeal haemolytic uraemic syndrome (HUS). [38] Since *Escherichia coli O157:H7* has been identified as foodborne pathogens, an increasing number of outbreaks [39-49] and cases [50-55] have been reported later after. Studies of diseases identifying and food inspections regarding *Escherichia coli O157:H7* were developing rapidly within Canada, British and America. [50-57]

E.coli O157:H7 infection has been reported all over the world. For instance, the rate of incidence is 8 out of 100 000 population or higher in areas of Scotland, [58] Canada, [59] and the USA [60]. South America also presents a high rate of people

infected by *E.coli O157:H7*, especially Argentina, where the incidence of infection with *E.coli O157:H7* is 5 to 10 times greater than the rate in North America [61, 62]. Additionally, people are easier to be infected by *E.coli O157:H7* in warmer months no matter in northern or southern hemispheres. This is because climate factors act as an important role and influence the rate of human infection.

E.coli O157:H7 could infect humans in many ways. First of all, animals and farmlands are major latencies for human to be infected by *E.coli O157:H7*. [60] That is because bacterium can exist in manure, paddy fields, and other areas on farms, [1] and the organism could also be isolated from wild animals. [1, 3] So, although a large number of human infections outbreaks happen in cities, people living in a country side also have a higher chance of infection, because villagers are more easy to use domestic animals, donkeys and castles, to do farm works. [63]

Pathogen contaminated foods could also transmit *E.coli O157:H7* from person to person. Most *E.coli O157:H7* outbreaks are related to human eating contaminated ground beef, raw milk, lamb and venison jerky, [4, 60, 64-66] since pathogen could arise from food processing such as slaughter, grinding and survive cooking. Most cases showed that pathogen could stay alive during fermentation and drying. [17]

In addition, there are growing numbers of outbreaks involved in vegetables and fruits contamination in the past few years. For example, baby carrots caused several outbreaks in Japan. [2] In U.S.A, fresh produce such as alfalfa sprouts, apple juice, and lettuce [67] have been involved in *E.coli*. pollution. Cross-contamination from meat products may also lead to outbreaks. Sprouts are most likely to be

contaminated by *E.coli O157:H7*, since the amounts of organism in seed may multiply during sprouting. [67]

E.coli O157:H7 infections caused by water that contributes to drinking[68] and swimming[69] in unsterilized water could not be neglected. Water cross-contaminated transmission happens in kindergarten and chronic-care facilities. [40, 70, 71] Infected by water or directly from person to person shows that low concentration of *E.coli O157:H7* could lead people to sick. One study suggested that fewer than 50 organisms could cause infection. [17]

2.2 PDMS Surface Modification for Nonfouling Applications

2.2.1 Poly (Dimethyl) siloxane (PDMS) Properties

Polydimethylsiloxane (PDMS) is a member of polymeric organosilicon compounds known as silicones. [72] At room temperature, a property of liquid form with high viscosity makes PDMS one of the most popular silicon-based organic polymers. The chemical and physical properties of PDMS are relative stable, such as optically clear, inert, non-toxic, and non-flammable. So, it can be used in many areas, such as biomedical, food inspection and chemical engineering.

Figure 1 shows the chemical structure of PDMS, where n is the number of repeating monomer [$SiO(CH_3)_2$] units. [72] After polymerization, solid PDMS surface shows a hydrophobic property. [73] This surface presents a mental luster, but the basement is clear. The surface structure, alkyl groups, keep PDMS getting away from being wetted by polar solvents such as water, and cause hydrophobic contaminants adsorption. Owing to the hydrophobic property of PDMS, PDMS can be applied for

storing or transporting alcohol and water solvents without material damage; however, most organic solvents, such as diisopropylamine, chloroform, and THF, will infiltrate into the substrate of PDMS and cause deformation. [73] Some organic solvents, such as acetone, 1-propanol, and pyridine, are compatible for instant use in PDMS microfluidic devices, as they lead to sufficiently small swelling.

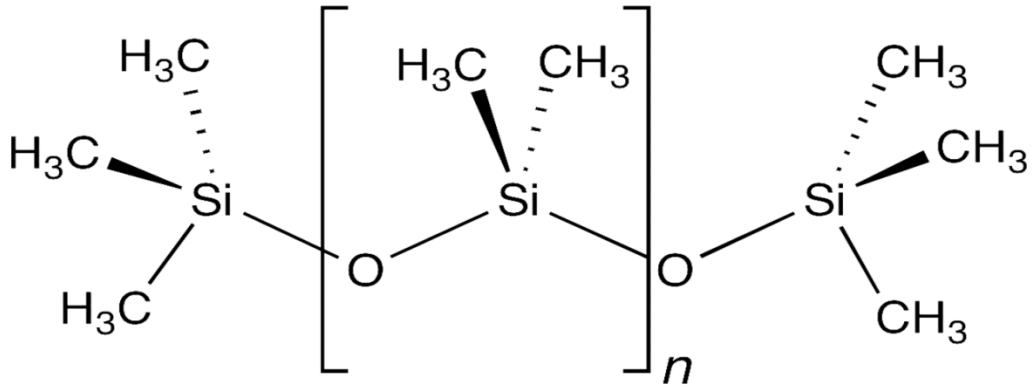

Figure 1. Chemical structure of PDMS, where n is the number of repeating monomer [$SiO(CH_3)_2$] units.

2.2.2 Soft Lithograph and Microfluidic Devices Fabrication

PDMS is one of the most commonly used substrate in microfluidics chips. [74] Generating an elastic stamp is a basic step of the procedure of soft lithography (figure 2a), which can stamp a few micrometers or nanometers sized patterns onto silicon based surfaces. With this method, it is possible to produce microfluidic devices used in the areas of food inspections or biomedical researches. The standardized methods of photolithography or electron-beam lithography can create this stamp. The resolution depends on the mask of the stamp and the highest resolution can reach 6 nm. [75]

In biomedical and food inspection systems, soft lithography is widely applied in microfluidic channels by transferring different chemical compounds into the device

both organically and inorganically. Most microchannels are designed onto silicon wafers and the wafers are covered by liquid PDMS and heat to harden. The microchannels will be imprinted on the PDMS when it is removed. With the treatment of plasma on the PDMS surfaces, the surface bonds are disrupted and the surface will changed into hydrophilic. A piece of glass slide is treated under the same conditions and is attached with the activated surface of the PDMS (the surface with microchannels). When the device is heated for 5 minutes, the glass will seal the PDMS permanently in a way by losing a water molecule, thus getting a waterproof microchannel (figure 2b). [76] Within these microchannels, research groups can use various of surface chemical changing methods to introduce functional groups to making special portable devices for rapid exam. [77]

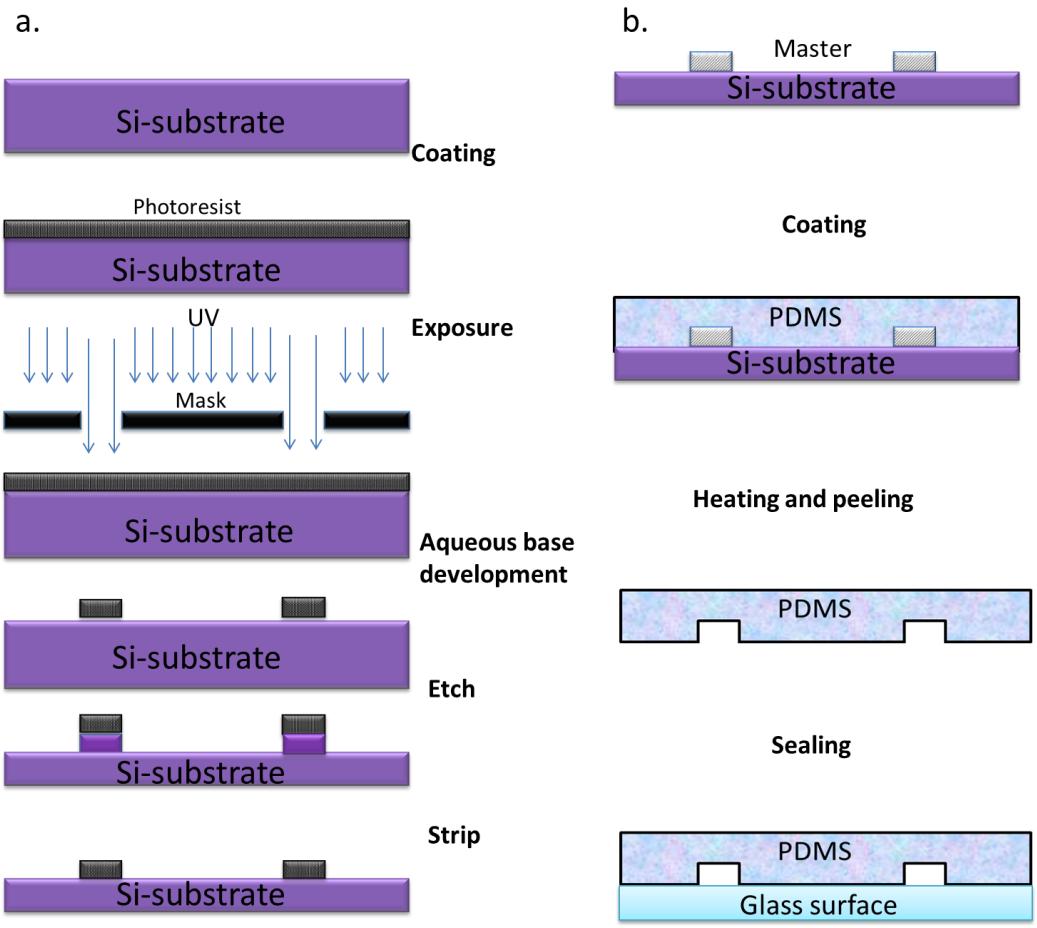

Figure 2. Soft lithography and microfluidic devices fabrication; a. soft lithography process; b. microfluidic devices fabrication.

2.2.3 Plasma Treatment of PDMS Polymer Films

Oxygen plasma can be used to change the surface structure of PDMS by introducing Si-OH groups to the surface. This method makes the surface of PDMS hydrophilic and to prevent the attachment of hydrophobic particles. Hydroxyl functional groups modified surfaces are stable for 30 minutes in air, after which the surface will gradually undergo hydrophobic recovery. [78] However, long time and high power exposing in plasma will damage the backbone structure, making lose efficacy of the modified surface. Normally, in optimum conditions, the seals strength can reach around 70 psi. [79] With the surface changes, the water contact angle

(WCA) often be reduced to be less than 5^{o} from its original 110^{o}. [79] In addition, N_2 plasma can also change the surface functional groups by introducing -NH_2 functional groups. This method is another suitable choice for PDMS surface modification. [32] Table 1 shows some typical gases used in plasma treatment and introduced functional groups corresponding to the gas types on different substrates. [80]

Table 1. Summary of types of gas and introduced functional groups in plasma treatment.

GAS OF PLASMA	INTODUCED FUNCTIONGROUPS OR REACTIONS	TREATED SBSTRATES
Oxygen plasma	Oxygen containing functional groups	Polymer surfaces such as PCL, PE, PET, and PDMS
Carbon dioxide plasma	Carboxyl groups	PP, PS, and PE
Air plasma	Oxidize reaction	PMMA
Ammonia and nitrogen plasmas	Amine groups	PTFE, PDMS and PS
Inert gases	Radical sites	PTFE, PE, PET, and PVDF

2.2.4 PDMS Surface Amination (silanization)

3-aminopropyltrimethoxysilane (APTMS) or 3-mercaptopropyltrimethoxy silane (MPTMS) secondary coating method was used to introduce more stable amino function groups. [32, 81-85] After oxygen plasma treatment, the chemical structure of APTMS can react with the hydroxyl functionalities to form a stable secondary layer (silanization reaction). The hydrophobic recovery time of APTMS coated surface can be over 14 days and the WCA is 63^{o} compared with bare PDMS surface 107^{o}. [86] Besides, the amino functional groups could provide favorable environment for biomedical researches. In many studies, researchers used amino modified PDMS surfaces for cell growth [86], because nitrogen-containing functionalities have been shown to improve cell attachment [87], and also amine functionalities could specifically capture some biomolecules such as enzymes and antibodies [88-90], DNA [91, 92], as well as proteins [88, 93-95].

2.2.5 Nonfouling Microfulidic Devices

Many studies have been done to prevent protein adsorption on PDMS surface. Vickers et al. [96] extracted unreacted oligomers and used plasma methods to increase the hydrophility of the microfluidic to prevent the hydrophobic particles absorption. Liu et al. [97] found that ionic polymers could prevent protein nonspecific absorption on microfluidic channels. Kyung at al. [98] developed a polyelectrolyte multilayers coated channels to avoid hydrophobic analytes absorption. Wirth et al. [99, 100]and Gezer et al. [101] successfully conjugated polyacrylamide brushes onto PDMS microchannels surface, and the result shows that nonspecific protein adsorption was significantly reduced. Using a new UV/Ozone pretreatment method, Stefano and his coworkers [102] grafted poly(poly(ethylene glycol)methacrylate)(PPEGMA) brushes onto the microchannels to prevent nonspecific protein attachment. However, these methods are complicated and the device performances are inefficient. For example, the unreacted oligomers method and the ionic polymers treated devices only show short time particles prevention ability due to a quick WCA recover rate. In addition, the polymer coating methods could not afford an extremely high rate of particle prevention, because the maximum nonfouling rate is only 10 times higher than the nonfouling rate of a glass surface [99, 100].

Three research groups used the polymer-modified methods to improve the performance into a higher level. Sasaski et al. [103] reported parylene coated microchannels to prevent fluorescent dye absorption. In this study, the researchers

used non-porous parylene transparent films to block the flaws on the PDMS surface and showed that the parylene coated microfluidic channels could prevent the absorption of RhB in a large scale. Other studies [18][19] proved that gases and organic solvents could not penetrate into the surface of parylene coated PDMS surface and this polymer could also be used to prevent the absorption of proteins and DNA molecules. Zhang et al. [104, 105] introduced 3-glycidoxypropyltrimethoxysilane and 3-chloropropyltrichlorosilane chemical compounds onto oxygen plasma-pretreated PDMS surfaces, and then grafted NH_2-PEG and alkyne-PEG linear polymers. The modification result characterized by Fourier transform infrared spectroscopy (FTIR) showing that two absorption characteristic peaks pointed at approximately 2880 cm^{-1} and 1338 cm^{-1}, corresponding to the $-CH_2O-$ groups of PEG. The modified surfaces were more hydrophilic in comparison with pristine PDMS (WCA: 70^o on the NH_2-PEG and 64^o on the alkyne PEG-modified PDMS surface, while control PDMS has a water angle around 108^o), and storage experiments showed that water wettability of the polymer modified surface was maintained for over 30 days. Recently, Yeh et al. [32] introduced the same polymer onto PDMS/SU8 based microchannels and they verified the surface properties and chemical composition by WCA, X-ray photoelectron spectroscopy (XPS), and atomic force microscopy (AFM). Subsequently, the researchers tested the efficacy the microchannel by the injection of florescent labeled bovine serum albumin (BSA) and manually counted the number of attached BSA from microchannel inlet to the end under a florescent microscope.

Finally the authors found that the nonspecific absorption could reduce 90% within PEG-coated microchannels compared with negative microassays. The reason of this phenomenon could be explained as the nonspecific adsorption caused by attractive interactions, such as hydrophobic interactions, van der Waals forces, and electrostatic interactions. As a result, if polymers have a long chain, the strong steric interactions that caused by the length of molecular chains can block the attraction force and reduce nonspecific attachment. In this case, PEG molecules have a larger hydration shells [81]. And also, in their paper, they emphasize that this PEG modification method could be further used in microcytometers, so that the microcytometers could be used in low concentration pathogens detection and reduce the influence of false negative results.

2.3 PAMAM Dendrimers

In the past decades, polyamidoamine (PAMAM) dendrimers have been widely studied in many fields, such as materials science and biomedicine. Dendrimers are nontoxic and free immunogenic. The compatibilities of dendrimers in organism make it possible for PAMAM to be used as drug delivery vehicles and tumor tracing markers. At the same time, the highly efficient cationic property of PAMAM enables dendrimers to act as vectors to deliver genetic materials into cells, and the “branch” structures are the best carriers for conjugating DNA oligos in biomedicine applications. In some researches, the dendrimers have been used as the coating agent on PDMS surface to avoid particle absorption, since dendrimers have a long chain structure and relative higher molecular weight. [30]

2.3.1 Dendrimer Synthesis

In early 1980s Tomalia et al. [106] first reported that they had successfully synthesized and characterized dendrimers. PAMAM are special synthetic polymers. Unlike straight chain polymers, PAMAM growth starts from a central core material such as benzene tricarboxylic acid chloride, ethylenediamine, ammonia or propyldiamine. It is very important to select the initiator core, as it will influence the entire chemical structure and surface electrification conditions. In traditional synthesis method, the growth of PAMAM molecule radiates form outside direction of the reaction core and PAMAM molecule will use a step-by-step polymerization reactions to grow based on former layers (generations) and finally the molecule will form a 3D branch-like structure. [107-109]

In synthesis of dendrimers, reaction methods include a Michael addition of methyl acrylate in the first step and an amindation reaction by ethylenediamine (EDA) in the second step. [108] The multistep reactions of PAMAM synthesis contribute new generations adding on the former generation. The generation is named by a continuous number (e.g. generation 0, 1, 2). The amino functionalities on the outside layer of dendrimers give the external surface of PAMAM molecule positively charge when PAMAM is exposed at physiological buffer. The layer can grow up to the tenth generation of molecule and stopped by steric hindrance, because the branch structure on the surface of each embranchment can inhibit the growth of other branches.

Two stage convergent methods could also synthesize PAMAM [110-112]. Firstly,

producing a dendrite by repeating connection of branch units. Secondly, anchoring a core on former productions, which can help the branch units grow into a multilayer dendrimers. Ideally, the perfect model of a PAMAM molecule performs a highly breached 3D structure with a spherical geometry. (Figure 3a) Purity of dendrimers is normally 98%, because synthesis procedures could cause small defects within branch structure. These flaws are normally caused by retro-Michaela additions and intermolecular lactam structure. [113]

2.3.2 Physical Properties and Characterization

The diametric scale of dendrimers ranges from 10 Å to 130 Å correspondingly from G0 to G10. [114] When a new layer is added on to the former layer, the molecular weight of PAMAM molecules will be increased dramatically, at the same time the amino functionalities on the dendrimers will be doubled and the diameter will be added around 10 Å (Table 2). [115] With the layer increase, the thickness of functional groups branching on the PAMAM surface will influence the polymer shape. When the generation number lower than G5, the PAMAM structure will present a 2D, elliptical shape; however, when the generation number is higher than G5, the structure of dendrimers will show a 3D, spherical structure [116]. (Figure 3b) it should be noticed that when the generation number is G4 or higher, the inner surface structure will change into a hydrophobic blank space which could be used as a capsule for drag deliver or other applications. [117, 118]

Table 2. Physical of characteristics of PAMAM dendrimers.

Dendrimer generations	0	1	2	3	4	5	6	7	8	9	10
Molecular weight	517	1430	3256	6909	14215	28826	58048	116493	233383	467126	934787
Primary amino functional groups	4	8	12	32	64	128	256	512	1024	2048	4096

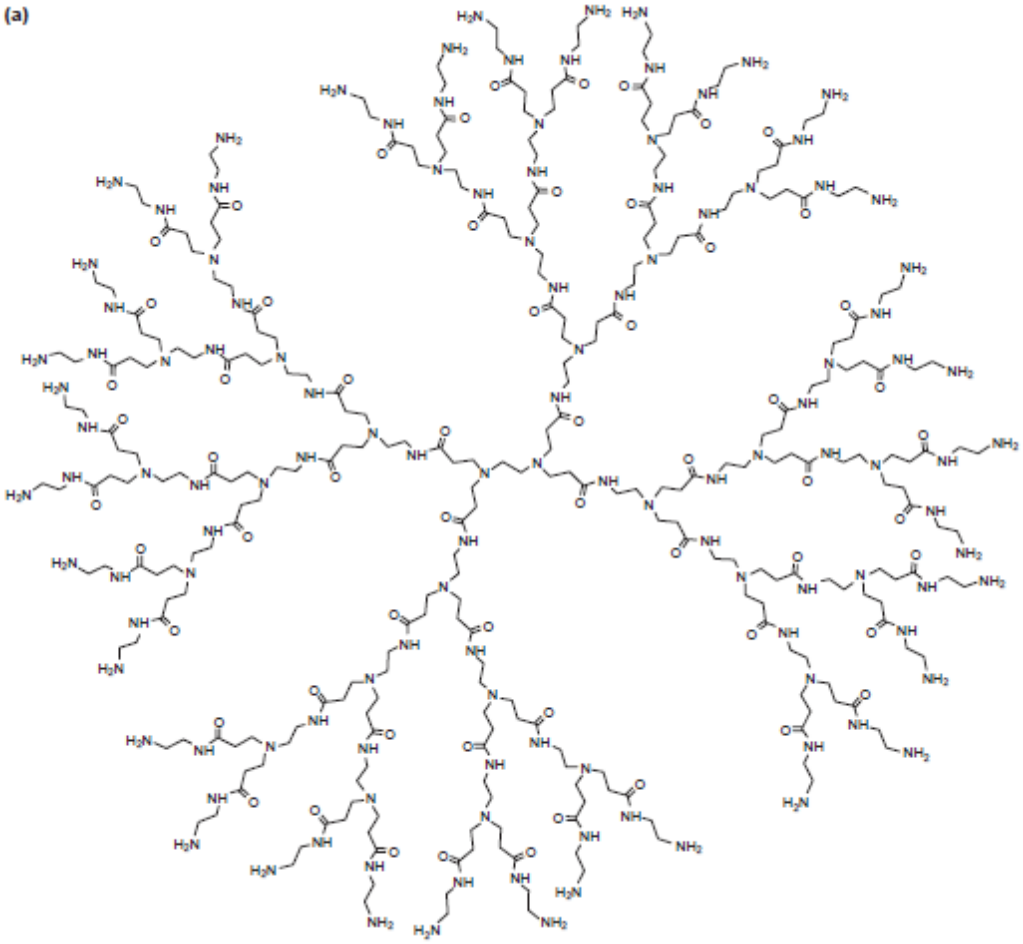

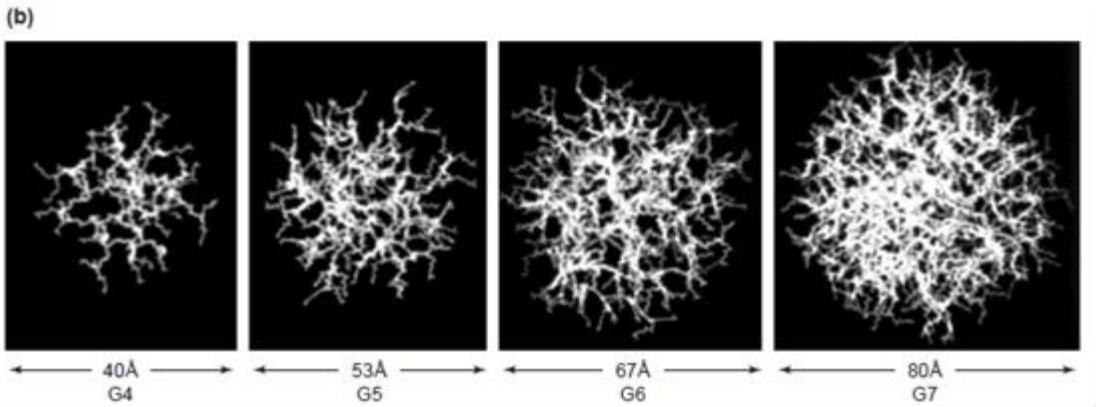

Figure 3. Structural characteristics of polyamidoamine (PAMAM) dendrimers. (a) Polymer growth emanates from the initiator core molecule in an outward direction by a series of polymerization reactions. As dendrimers grow in generation, they become highly branched polymers with internal cavities capable of holding small organic molecules. Dendrimers also have a high number of primary amine surface groups, which enable the polymer to interact electrostatically with nucleic acids. (b) Molecular modeling of PAMAM dendrimers [generation 4 (G4)–G7].

Several methods could characterize PAMAM dendrimers, such as NMR with ^{31}[P], ^{15}[N], ^{13}[C] and ^{1}[H], electrospray–ionization mass spectroscopy (ESI–MS), size-exclusion chromatography (SEC), capillary electrophoresis, electron paramagnetic resonance (EPR), gel electrophoresis and high-performance liquid chromatography (HPLC) [108, 119-122]. Researchers often combine analytical methods mentioned above to draw a precise conclusion about the chemical and structure compositions on PAMAM dendrimers. Commercial PAMAM dendrimers are processed under a standard procedure and provide a stable chemical property for many applications. Many researchers have used dendrimers to modify surfaces and tested these surfaces by AFM. [123-125] As shown in Figure 4. Li et al. [124] have studied G5 to G10 PAMAM conjugated surface using AFM, and the molecular weights and volumes calculated were in accordance with theoretical values. These tests evidently prove the morphology and thickness of these dendrimers.

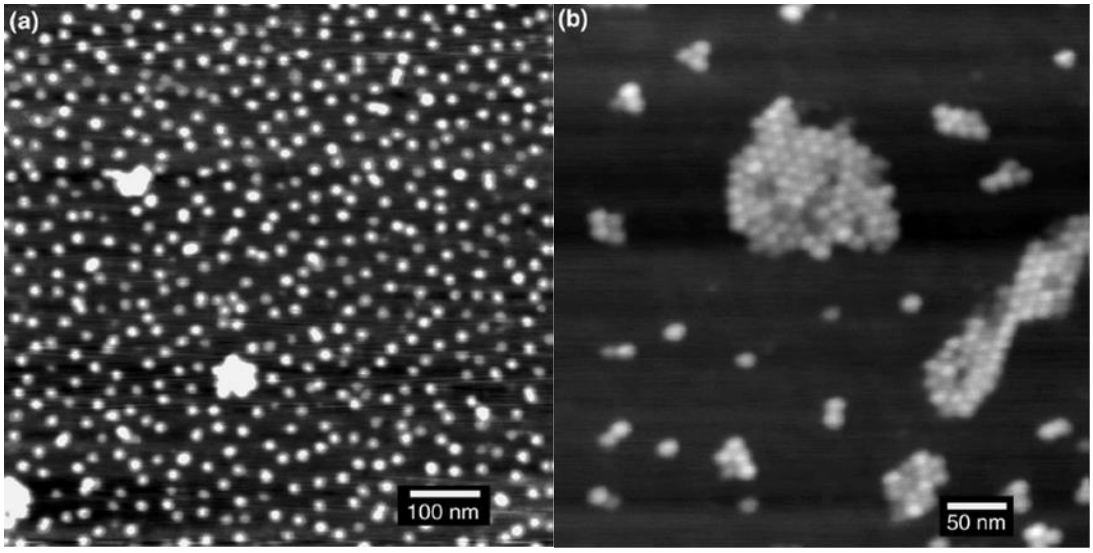

Pharmaceutical Science & Technology Today

Figure 4. Atomic force microscope (AFM) images of generation 9 (G9) ethylenediamine (EDA) dendrimers. (a) G9 EDA dendrimers uniformly spread on a mica surface after air drying. (b) Formation of G9 EDA dendrimer aggregates on mica surface after the solute (water) was wicked off with filter paper.

2.3.3 Poly(amidoamine)-succinamic Acid Dendrimers Synthesis and Characterization

In many researches, amino terminated PAMAMs should be transferred to carboxyl terminated PAMAMs in order to conjugate with small amino modified biomolecules such aptamers, antibodies and RNAs. Xiangyang et al. [126] and Srinivas et al. [127] used a standard protocol through succinamic acid to synthesis carboxylic PAMAMs, as shown in Scheme 1. Compared with amino terminated dendrimers, COOH-PAMAMs have following advantages: 1. it is much easier to modify and control. 2. The number of carboxyl fictional groups on the COOH-PAMAMs stays the same as that of the former amino terminated PAMAMs, which is an important factor for calculation of PAMAM related chemical reactions.

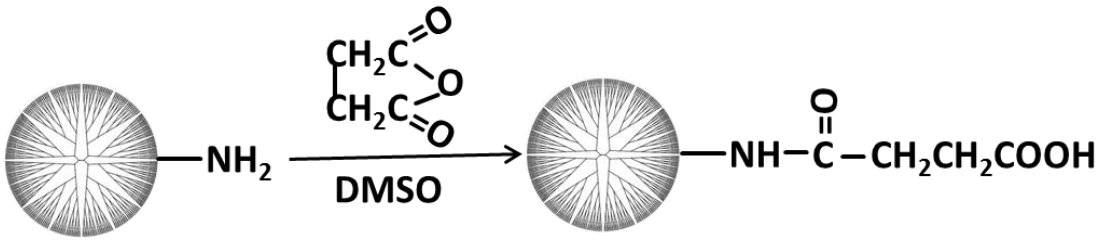

Scheme 1. Schematic representation of the synthesis of PAMAM-SAHs.

2.3.4 Dendrimer DNA Conjugation

Dendrimers have much more sable structures and show the precise geometry of design. Their properties of nontoxic, biodegradable negatively charged surface and changeable surface functionalities make it possible for dendrimers to conjugate with DNAs in many research fields, such as gene therapy, cancer cell labeling, and DNA based biosensors. In the early stage, the dendrimers-DNA conjugation was used to infect target cells. [128, 129]

Electrostatic interactions between negatively charged backbone structure of DNAs and the positively charged amino functional groups on the surface of dendrimers generate dendrimer-DNA conjugation called dendriplex. The dendriplex could bind to cell surface, at the same time, under the interaction of the positive charges of lipid and carboxylate of the cell membrane, the dendriplex can be taken up into the cytoplasm and can target the cell nucleus. [130] So, these behaviors of dendriplex can be used in gene therapy, because the dendriplexs act as vectors, and the vectors can transport desired genes into cells to correct genetic defects. [131-133]

Apart from infection of cells, DNA-dendrimer complex can also be used as detections probes to detect and labeling target cells. Liu et al. [29] used covalent

binding of COOH-G4 with amino functionalized DNA oligos, and this nano-complex could use DNA as a template to locate the targets. They concluded that the covalent coupling method is reliable, efficient, and fast, so the nano-complex has the potential in using cell tracing. The same strategy has also been used in Li et al. [28] where the researchers used thiolated PAMAM dendrimers to conjugate with DNA and quantum dots (QDs) complex creating a nontoxic and water soluble nanomaterial. After, they used gel electrophoresis to separate the components and applied ^{1}H NMR spectra to test their materials. In a future step, the PAMAM-QD-DNA nanoprobes were bind with U251 glioblastoma cells. Finally, the florescent results showed the nanoprobes can bind the target cells specifically.

Another application for DNA conjugated with PAMAM is dendritic DNA based biosensors. The theory of DNA microarrays and biosensors often consists of locating PAMAM-DNAs on glass slides through covalent links to test complementary fluorescent labeled analytes where fluorescence is served as quantifying indictor. Many research groups [134, 135] have largely improved the glass surface by planting of dendrimers and DNAs in order to increase the performance of sensors. For example, Niemeyer group [8, 136] firstly used PAMAM dendrimers to change the glass surface and to conjugate DNAs which after DNAs labelled by fluorescent complementary ones. The result showed more stable and higher fluorescence intensity than other control groups, because dendritic linkers can bind more fluorescence. Subsequently, more groups changed traditional modification methods [26, 137-139] by increasing the generation of dendrimers, changing the functional

groups into aldehyde terminated and binding the dendrimers onto aminated slides. As the result, the sensor has provided a better performance. Additionally A G3-PAMAM dendrimer biotin glass base sensor using avidin to detected low concentration of DNAs has been developed. [138] The chip was examined by AFM and SEM and showed a favorable performance.

2.4 Antibodies VS. Aptamers

For over the last four decades, antibodies were the most popular biomolecules in the world for applications in the field of molecular recognition. As a result, the invention of most diagnostic tests in clinics and the improvement of diagnostic assays, which are commonly used today, were based on the contribution and development of antibodies. [33]

Aptamers emerged with the enhancement of the systematic evolution of ligands by exponential enrichment (SELEX) process has changed the time that antibodies dominated the development of therapeutic and diagnostic technologies. [33] That is because SELEX technologies could isolate oligonucleotide sequences to create biomolecules, aptamers, which could recognize almost any type of target object with high affinity and specificity. Aptamers differ from antibodies, but aptamers can imitate functions of antibodies in most of diagnostic methods. [20] Over the 20 years development, aptamers related technologies have been developed into sophisticated methods. Many aptamers based detection devices have been sold in the market, and in such devices, aptamers are gradually replacing the role of antibodies. [20]

2.4.1 Antibodies

When we discussed about diagnostic devices, we could not ignore the functions of antibodies. In terms of technologies and applications of molecular recognition, antibodies have made great contributions. The first usage of antibodies to detected analyses could date back to the 1950s [140]. In the 1970s, antibodies became commonly used because they can be extracted from polyclonal serum in immunized animals. However, researchers need a lot of preparations for producing a large amount of antibody by polyclonal antibody methods. Hence, the number of produced antibodies could not meet the demands for immunological assays until Kohler and Milstein [141] created monoclonal antibody methods for producing a simplex antibody with great amount. Later, this technology became very popular and utilized by scientists around the world. In processing, producers use cell culture methods to create monoclonal antibodies and sufficient quantities is required, because antibodies are easy to operate in detection devices and florescent based detection methods. Nowadays, people use select clone method to produce a selected monoclonal antibody constantly. Theoretically, the number of produced antibody can increase infinitely with the unlimited cell culture nutriment for an antibody growing. Moreover, there is no need to purify immunogen, which is used for recognizing monoclonal antibodies. The above mentioned methods are some monoclonal antibody methods, as they have improved the development of immunology and widen the usage of antibodies.

However, the disadvantages of antibodies are obvious too. [33] Firstly,

antibodies generation process start with in vivo environment, so it is difficult for antibodies to be selected against molecule that are weakly immunogenic and intensively toxic, such as toxins. [33] Secondly, the process of hybridomas is coming from murine, which limits the usages of antibodies in therapy and diagnosis. For example, in some cases, heterophilic antibodies have tendency to conjugate with a secondary antibody structure (a capture antibody non-human origin link with indicator antibody) when there is no target analyte, causing a false-positive result. [33] Thirdly, the processes of monoclonal antibodies production is labor intensive and time consuming. Fourthly, the antibodies selection process is limited in vivo conditions, so harsh conditions and non-physiological environment cannot be applied for the selection of antibodies. Finally, antibodies are temperature sensitive biomolecules, and the thermal denaturation process is irreversible. For example, the antibodies interleukin-1 will be perpetually denatured when the temperature is higher than 53.5^{o}C. [33]

2.4.2 Aptamers

Aptamers are single-stranded highly structured oligonucleotides, which can be selected by SELEX technology from a random DNA or RNA library. Aptamers have high affinity and are specific to their targets in a various ranges of molecule size [142, 143]. Due to their specificity, high affinity and good stability, aptamers can replace antibodies in many research fields, such as biosensors, bio-imaging and aptamer-based affinity purification [144, 145]. Additionally, aptamers are excellent biomolecules for clinic diagnosis, analytes detection, recognition and separation. For

example, many researches show that aptamers related analytes can vary significantly including, metal ions, proteins, amino acids, peptides and cells. [143-145] Moreover, the obvious advantages of aptamers complement the disadvantages of antibodies, so these merits make the applications of aptamers have a better prospective in analytical areas. These merits are listed below. [33]

Firstly, aptamers are synthesized in a vitro condition instead of in vivo, so the chemical structures of aptamers can be changed by research requirements. Secondly, aptamers can be processed with desirable properties that are suitable for diagnosis, and aptamers can be screened for nearly any type of molecules, even the molecules have toxicity or have poor performances in immune responses. Thirdly, the rate of aptamers to conjugate on the target molecules can be controlled. Fourthly, batch to batch variation has little influence on the properties of aptamers, because aptamers are processed with a standard chemical procedure leading to high accuracy and repeatability, meanwhile, purification processed under denaturing conditions makes aptamers become super pure. Fifthly, marker molecules, such as fluorescence dyes and biotin, can be added to the desired spots of aptamers chosen by the researchers, and diverse functional groups can be also attached on the chain of the aptamers at different locations during the synthesis without changing their affinity. Sixthly, the small size enables aptamers to conjugate with nano-size materials. Finally, aptamers can be recovered in a few minutes after denaturing condition, so aptmers can be used in PCR and are stable in long-term storage at ambient temperature.

2.5 Microfluidic Channels for Rare cell Detection

Compared with traditional pathogen detection methods, microfluidic detection method is faster, portable and more accurate. As a result, in the last two decades, microfluidics has gained the popularities. Many novel inventions in this area have been created to detect various types of pathogens. With such developments, recently, researchers have focused their attentions to make a more advanced microfluidic system. The system will generate all the detection steps on one chip with high work performances and detection sensitivity. There are some common features involved in their creations. So, in this part, we will conclude some commonly used microfluidics and a common detection method for bacterial detection.

2.5.1 PCR Based Microfluidic for Rare Cell Detection

PCR technologies have been widely used in detection of pathogens for clinic diagnose, so researchers use its sensitivity combining with microfluidic system to increase the performances of the microdevices. [9, 146] But, normally, the LOD of a DNA based microfluidic system is only 10^5 cells/ml. [147] In general, PCR on microfluidics can be classified into three types [147]: 1.immbolized-tank PCR reaction microfluidic channels. Traditional thermocycling PRC reaction could react in these tanks. 2. Reaction zones microfluidics, which are suitable for continuous PCR reactions with various temperatures at these spots. 3. Water drops microfluidics. The PCR reactions are released drop-by-drop and controlled by the droplets (oil coveres with water droplets). However, the biggest problem for this device is that the nonspecific absorption of the channel surface, which prevent the

PCR reaction.

2.5.2 Antibody Based Microfluidic for Rare Cell Detection

Another useful detection method for bacteria inspection involves immunological technologies. It depends on the specific interactions of proteins to proteins, proteins to carbohydrates or proteins to DNAs [6]. Antigen and antibody identification systems are commonly used in pathogen detection. There are many examples to show that this method can detect different pathogens in a various cell concentrations.

Bouvrette et al. [148] have used an antibody immobilized chip to detect *E.coli*. compared with other approaches, this method can determine cells without any labeled compound, because the method is directly detected the cell's b-D-glucuronidase (GUD) activity. The results show that antibody can identify *E.coli* specifically even if there are existence of Shigella boydii and another GUD-positive bacterium, and the LOD can reach 10^5 cells/ml, which is lower than a normal level 10^6 cells/ml.

Many other approaches combine magnetic particles and antibodies to achieve automatic detection process. This microfluidic system has been used for detection of many pathogens such as, *B. anthrax spores, E. coli O157* and *S. typhimurium* [149-152]. There are many advantages for this method: 1. the detection process are more repaid and can be automated. 2. It is a continuous process, so human influences for the detection are less. 3. The read out format can be programmed by a detector linked with a computer, so it is much more reliable.

Perez et al. [152] used amperometric microfulidic system to detect *E. coli O157* and the LOD was 10^5 cells/ml. In their approach, they used antibody immobilized microbeads to capture the *E.coli*. After, redox mediators were introduced into the system, and when it reacted with the *E.coli* which was captured by the antibodies, current signals could be changed and finally the cell concentrations would be detected. Abdel-Hamid et al. [153] decreased the LOD to 50 cells/ml and reduced the detection time to 40 minutes by using an amperometric microchannel system. In their approach, they immobilized antibodies on a Nylon membrane were attached on a carbon electrode. When the buffer with *E.coli* goes through the Nylon membrane and then pass the microchannels, signals which were different from the original ones will be detected by a counter and calculated by a computer. And this system can be easily used for the detection of other foodborne pathogens like *Salmonella*. A further experiment proved that the LOD of *Salmonella* can be also reached to 50 cells/ml and the detection time was 35 minutes, when Abdel applied with this approach.

2.5.3 Aptamer Based Microfluidic for Rare Cell Detection

Compare with traditional microfluidic systems, aptamers based microfluidic systems are more sensitive. [20] The unique properties of aptamers based microchannels in saving analysis time and process simplification win the potentials for real sample detection. There are lots of articles talking about this field. In the followings, we will show some specific examples that are related to our project and compare some typical aptamer based microfluidics in target detection.

Tan et al. [154] conjugated aptamers in a microchannels to catch rare cells and realized fast detection without any preprocessing (Figure 5).Their method has showed high engraftment purity (97%) and excellent capture performance (80%) respectively. They predicted that their microfluidic system could detect multiple types of cancer cells at the same time. Soper et al. [155] have developed an aptamer-enriched microchannel to capture low concentration cancer cells specifically. In their method, prostate-specific membrane antigen (PMSA) identifying aptamers were screened and coated onto the surface of a microfulidic and the device was combined with a sensitive sample collecting machine. Results showed that the detection sensitivity could reach to 90% for rare circulating prostate tumor cells collected from peripheral blood matrix. Swensen groups [19] have created an aptamer-based electrochemical microfluidics. In their study, they used cocaine related aptamers and conjugated them on the surface of the microchannel and the theory of the detection is based on the changes of conformation of target objects and the aptamers, because when the aptamers bind with targets, the electrochemical signal will be changed due to the structure changes of aptamers, and the electric signal will be received by the acceptor. The results showed that the device could detect blood serum contains cocaine molecules in the physiologically conditions. Huang et al. [156] modified magnetic microparticles with aptamers and the microparticles conjugated with the analytes adenosine, was injected in to the microfluidic channels. The stream of magnetic microparticles could be changed by magnets guiding them to touch the surface of the microchannel, and the capture

agents on the channel surface could specifically link with these particles. Finally, the signal will be detected by a magnetic detector. Therefore, in their researches, all of them demonstrate that the aptamers have great potential to be used in the microfluidic system, and using aptamers as the targeting capturing molecules could provide a high specificity and fast binding properties. Moreover, aptamers are suitable for detection complicated samples in non-physiological conditions. In addition, the methodologies for aptamers conjugated on microchannel surfaces vary from physically methods to chemical methods. The design and modification of aptamers could satisfy the usage of different types of microchannels such as, optical based micochannels, electrochemical based microchannels and microparticles magnetic based mirochannels.

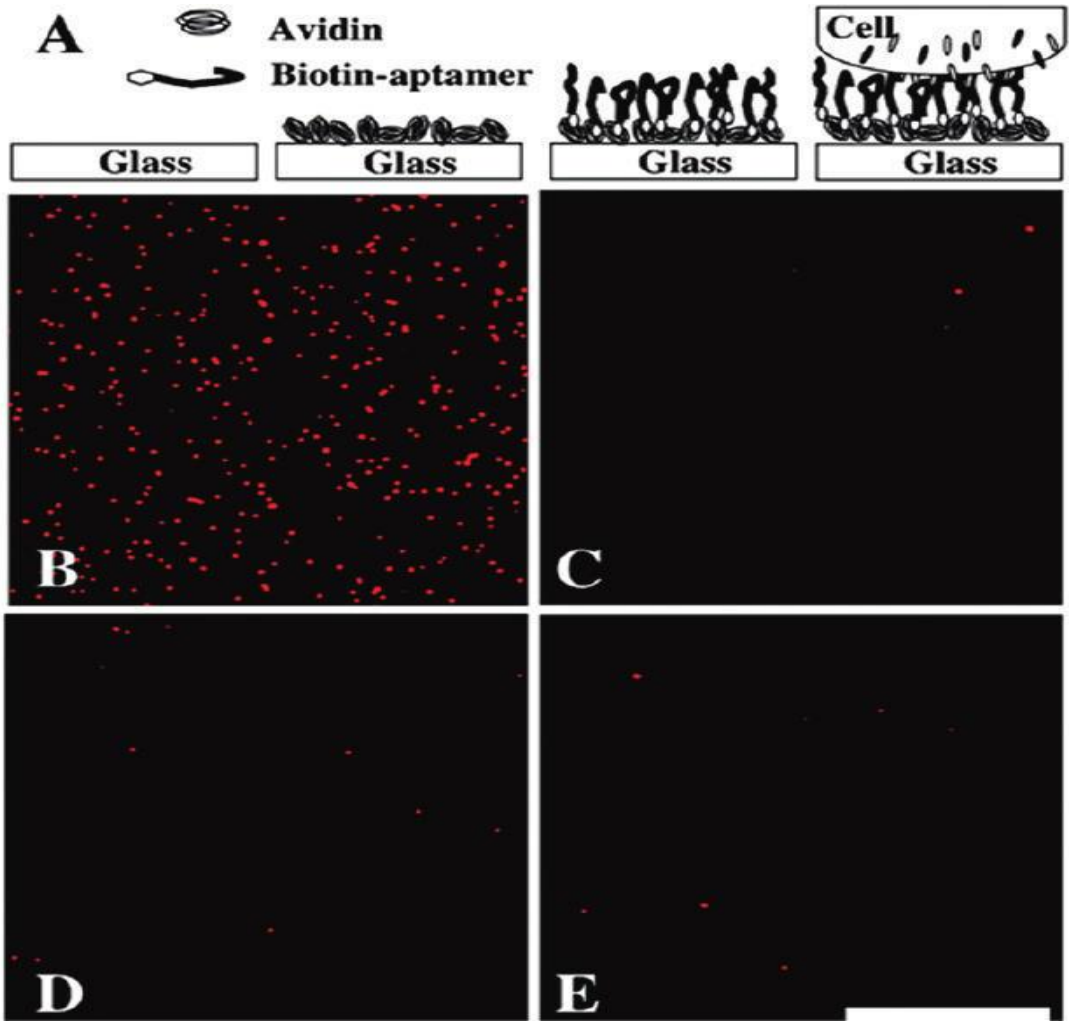

Figure 5. Aptamer-based capture and enrichment. Reprinted with permission from [154]. Copyright (2009) American Chemical Society. Immobilized sgc8 aptamer was used to capture its target cells. (A) Schematic representation of the aptamer immobilization and target capture. (B) Specific capture of the target cells using the sgc8 aptamer. (C) Representative capture of the control cells using the sgc8 aptamer. (D) Capture of the target cells using immobilized random DNA sequence. (E) Capture of the control cells using immobilized random DNA sequence.

Most importantly, for some groups, they combined aptamers with dendrimers and applied them into the microfluidics, which are similar to our study. For example, Zhou groups [157]have created an aptamer–dendrimer based microfluidic. The hybrid nanomaterial mimics antibodies structurally and functionally. In their study, there were two steps. Basically, in the first step, they used chemical methods to link

aptamers onto surface of dendrimers; and in the second step, they created interactions between two adjacent aptamers generating antibody-like-structure hybrid aptamers (Figure 6). In this method, the hybrid structure act as the binding sites of an antibody to link with an antigen, and the dendrimer carried fluorophores was regarded as a detection probe. When the hybrid nanomaterial was incubated with the target cancer cells solution, it could specificity conjugate with the analytes in a high binding affinity. Because dendrimer is a multi-branch polymer, theoretically, dendrimer molecule can conjugate to large numbers of aptamers, which have potentials to improve the detection sensitivity of microfluidics.

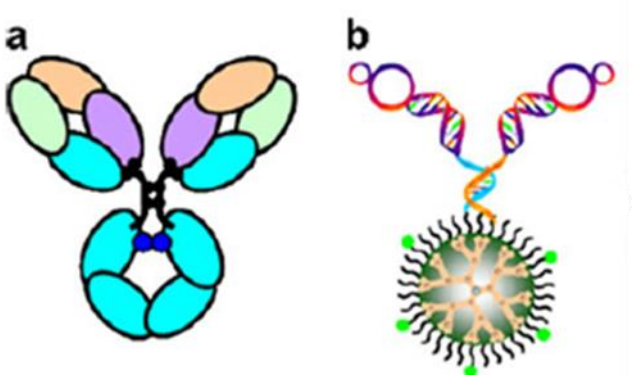

Figure 6. The nanostructure of a natural antibody (a) and an antibody mimic (b). The antibody mimic is a bivalent aptamer–dendrimer nanomaterial. Copy right Springer; accepted from [153]

In Table 3, Xu group [20] concluded the applications of the aptamers based microfluidics and classified in various roles of apatamers played in microchannels. Specifically, they can be classified into four types. As for electrophoresis microchips, the merit could be time-efficient and accurate, but the machines for detection are often very big and complicated and people need to calculate the detection figures. Another type is aptamers for miniaturized affinity chromatography, in which targets could be detected in a small machine, but the accuracy of detection is not as high as

electrophoresis microchips and the time for detection is relatively longer. The simplest type of microfluidic system is sandwich structure chips. It is very fast but the detection efficiency is relatively low. The last type of microchips is temperature responsive sensors. The structure of aptamers could change according to different temperatures, so it can achieve to catch and release the targets by controlled temperature. However, the researches in this field are limited. Hence, aptamers are replacing antibodies in the field microfluidics gradually. Meanwhile, aptamers exhibit many merits in their applications such as more sensitive, accurate and money-saving, and they are also compatible for many detection methods, such as fluorescence detection, electrochemical detection and mass spectrometry. These advantages of aptamers help microfluidics to reduce the LOD in a large scale. It is suggested that the aptamers will be developed rapidly in the field of microfluidics in the future.

Table 3. Summary for various applications of aptamers in affinity microfluidic chips.

Types of aptamers in applications	Detection methods	Target analytes	Real samples	Limit of detection	merits	Ref.
Probes in microchip electrophoresis	Laser induced fluorescence	Thrombin	Rabbit, human plasma	543.5nM	Simple, efficient, real-time, unlabeled target	[158]
	Laser induced fluorescence	VEGF(165)	Rat blood plasma	1.0nM	Fast, low reagent consumption, high separation efficiency	[159]
	Laser induced fluorescence	Natriuretic peptides	/	/	Improved performance, speed, and cheap	[160]
Aptamers for miniaturized affinity chromatography	Mass spectrometry		Hepatitis C patient serum	9.6 fmol		[161]
	Fluorescence detection	HCV RNA polymerase	Protein mixture	170 fmol	Effective purification of the target protein, preventing the protein from contamination	[162]
	Chemiluminescence detection	C-reactive protein	Not available	0.0125mgL−1	Fast, accurate, sensitive, reduced reagent consumption	[163]
	Love-wave sensor	α-Thrombin, HIV-1 Rev peptide	Not available	72±11 $pgcm^{-2}$(Thrombin),77±36 $pgcm^{-2}$	Label-free, real-time, easily regeneration	[164]
	surface acoustic wave sensor	Thrombin	Not available	Not available	Highly specific and sensitive	[165]
	Confocal microscope	Cancer cells	Cell mixture	Not available	>97% purity, >80% efficiency, completed within minutes and no pretreatment	[166]

Types of aptamers in applications	Detection methods	Target analytes	Real samples	Limit of detection	merits	Ref.
	Bright field and fluorescence microscopy	Circulating prostate tumor cells	Whole blood	Not available	High recovery (90%), high purity (100%), 100% detection and sampling efficiency, high-throughput, no labeling approach	[155]
	Comparative unbinding force assay	Adenosine	10% fetal bovine serum	53.5 μM	Label-free, excellent selectivity	[167]
	Electrochemical detection	Cocaine	Undiluted blood serum	Not available	Continuous, real-time (~1min time resolution)	[19]
Aptamers for sandwich structure chips	Fluorescence detection	Thrombin	Not available	10μgL^{-1}	Simplified washing, facile automation, rapid, reduced reagent consumption	[168]
	Electrochemical detection	Thrombin	Human plasma	1pM	High sensitivity and specificity, favorable for the detection of real samples	[169]
Temperature responsive sensors	Mass spectrometry	AMP	A sample mixed with nonspecific analytes and contaminated with salts	10nM	Enhanced enrichment (by ~100×), detection of analyte at trace levels	[170]
	Fluorescence detection	TO-AMP	Intermixed with non-target compounds	1 pM (possible)	Selective extraction, efficient analyte release and device regeneration, simplistic fabrication, elimination of harsh solvents	[171]
	Mass spectrometry	AVP	Mixture of AVP and AMP	1 pM	Ultrasensitive, rapid, uncomplicated, free of chemical	[172]

Chapter 3. Experimental

3.1 General Approach.

In this study, we report our new approach to prepare a microfluidic device for sensitive foodborne pathogen detections. As shown in Figure 7, the microchannel device is initially treated with oxygen plasma, which is followed by microchannel amination by APTMS treatment on the PDMS surface [32]. Subsequently, PAMAM dendrimers are immobilized on the aminated surface to enhance its nonfouling performance and at the same time to provide multiple handles for further aptamer modification on the surface for bacteria detection. To test the efficacy of this approach, fluorescently labelled *Escherichia coli O157:H7* cells are used as model target cells for detection.

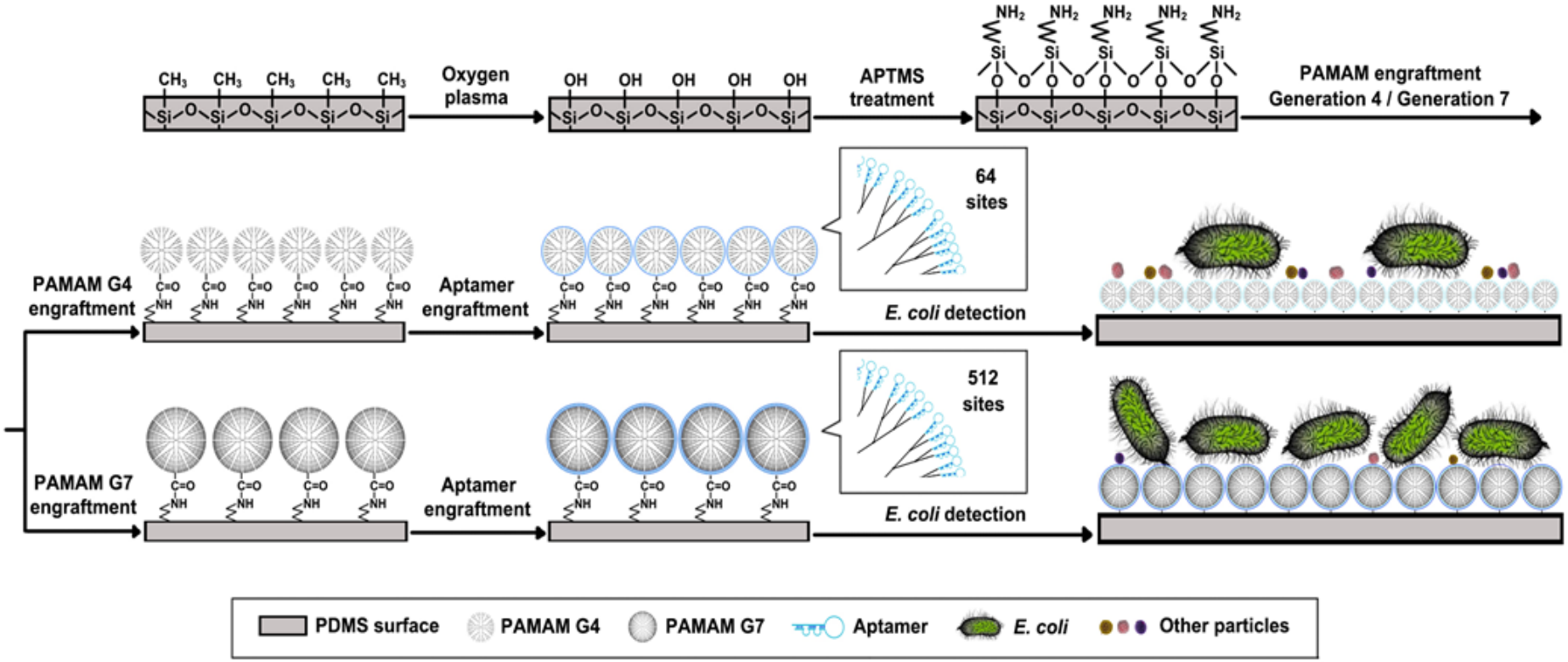

Figure 7. Illustration of the general approach for fabrication of PAMAM-aptamer grafted PDMS and *E.coli* detection methods.

3.2 Materials

PAMAM dendrimer (generation 7, PAMAM-G7) and PAMAM dendrimer (generation 4, PAMAM-G4) were purchased from Sigma (Oakville, ON). Furthermore, both G7 and G4 PAMAM-NH_2 were functionalized with carboxyl groups (i.e. PAMAM-COOH) using a method described elsewhere [126, 173] (see Supporting Information for more information). A Sylgard 184 PDMS kit was obtained from Dow Corning (Midland, MI). SU-8 negative photoresist was purchased from MicroChem (Newton, MA). N-hydroxysuccinimide (NHS), NHS-rhodamine, (3-aminopropyl)-trimethoxysilane (APTMS), and 2-(N-morpholino)ethanesulfonic acid (MES) were obtained from Fisher Scientific (Ottawa, ON). 1-(3-Dimethylaminopropyl)-3-ethylcarbodiimide (EDC) was purchased from Alfa Aesar (Ward Hill, MA). Anhydrous ethyl alcohol was purchased from Commercial Alcohols (Brampton, ON). Nuclease-free water and IDTE Solution (1×TE, pH 7.5) were obtained from Integrated DNA Technologies (Coralville, IA). Heat killed FITC-labeled *E coli* O157:H7 was a generous gift from the Canadian Food Inspection Agency (Ottawa, ON). All aptamers used in this study were obtained from Integrated DNA Technologies (U.S.A), and their sequences are listed below:

Aptamer for *E.coli O157:H7:* [174]

5'/5AmMC6/CCGGACGCTTATGCCTTGCCATCTACAGAGCAGGTGTGACGG 3'

Disarray aptamer: [174]

5'/5AmMC6/GCCGGCTCAGCATGACTAAGAAGGAAGTTATGTGGTGTTGGC 3'

Cy3-aptamer:

5'/5AmMC6/CCGGACGCTTATGCCTTGCCATCTACAGAGCAGGTGTGACGG/3Cy3Sp / 3'

3.3 Methods

3.3.1 Surface Amination and Characterization

a. PDMS Surface Amination

To introduce amino groups to the PDMS surfaces, we used a method as we previously reported with minor modifications [32, 175]. Briefly, a PDMS surface was treated with oxygen plasma using a plasma cleaner (Model SP100, Anatech Ltd, Battle Creek, MI) at 100 mTorr, 118 W for 10 s. Immediately after the plasma treatment, the treated surface was soaked in APTMS solution (5 wt % in anhydrous ethyl alcohol) for 30 seconds, after which the excess APTMS solution was removed from the PDMS surface by compressed air. Finally the aminated PDMS surface was left to dry for at room temperature 30 min.

b. Characterizations of Surface Amination

To confirm the success of PDMS surface amination, an Agilent FTIR (Cary 630, Agilent Technologies) was used. Three sample surfaces were characterized: native PDMS surface, PDMS surface treated with APTMS only, and PDMS surface treated with both oxygen plasma and APTMS.

Furthermore, in order to evaluate the extent of the PDMS surface amination, a well-established fluorescent labelling technique was employed [32, 176-178]. The

surfaces of interest were fluorescently labeled with -- via surface primary amines -- rhodamine-NHS, and the relative intensity of fluorescence emitted by the labeled surfaces was measured. This method is an approximate approach for evaluating the relative amount of functional groups of interest on a surface. Briefly, in a typical experiment 10 mg/mL rhodamine-NHS in anhydrous dimethylformamide was mixed with PBS (pH 7.4) at a proportion of 500 μL PBS per μL rhodamine-NHS DMF solution. The resulting labeling solution was used to react with the surfaces of interest at room temperature for 30 min, after which the surfaces were washed using PBS (pH 7.4) at a flow rate of 0.05 mL/h for 10 min and stored in PBS (pH 7.4) for future analysis. To analyze fluorescence intensity on the surfaces, fluorescence images were first captured by an inverted fluorescence microscope (Olympus IX81, Richmond Hill, ON) equipped with a high-resolution camera (QImaging, Surrey, BC) and the original color images were converted to gray-scale and analyzed by Image-Pro Plus 6.0 software (Media Cybernetics Inc., Rockville, MD). The fluorescence intensities of the unmodified surfaces before amination were used as controls.

3.3.2 PAMAM Surface Immobilization and Characterization

a. PAMAM Surface Immobilization

To immobilize PAMAM onto PDMS surfaces, amine functionalized PDMS surfaces were incubated with 4.0 μM PAMAM-COOH (details in Appendices A1), 1.74 mM NHS and 1.04 mM EDC in 0.1 M MES solution (pH 6.0) at 30 °C for 2 h. The

surfaces were subsequently washed using PBS (pH 7.4) to remove unreacted reagents and finally stored PBS (pH 7.4) for further analysis.

b. PAMAM Immobilized Surface Characterizations

To confirm the success of PAMAM surface immobilization on the PDMS surfaces, the following surface characterization methods were used [32, 175].

Water Contact Angle Measurements. To investigate PAMAM surface modifications, water contact angles of surfaces of interest were characterized using a goniometer (AST Products Inc., Billerica, MA). For each sample surface, three measurements (2 readings per measurement, total of 6 readings) were taken at random locations on a sample surface, and the averaged values were reported.

Characterization of PAMAM Engraftment. To further study PAMAM engraftment, surfaces were characterized by an X-ray photoelectron spectroscopy (XPS) (PHI 5500, Physical Electronics, Chanhassen, MN). The take-off angles for all measurements were fixed at 45 °. For all XPS analysis, 285.0 eV was used as a reference position for C-H(C) peak in this study. High resolution spectra C 1s and N 1s peaks were analyze by XPSPEAK software Version 4.1.

AFM Surface Analysis. Morphology changes of the modified surfaces were monitored using a Veeco Di Multimode V atomic force microscope (AFM) (Santa Barbara, CA). Surfaces of interest were characterized in contact mode, and the obtained data were further analyzed by a NanoScope software (Veeco, Santa Barbara, CA).

3.3.3 Aptamers Engraftment

To further immobilize aptamers on the PAMAM modified PDMS surfaces, the PAMAM modified surfaces obtained from above mentioned experiments were activated by 5.2 mM NHS and 0.26 mM EDC in 0.1M MES solution (pH 6.0) for 1 hour at room temperature and washed 10 times with nuclease free water. The resulting surfaces were incubated with 100 µl 10 µM aptamer (5' ends capped with amino groups) IDTE buffer solution (pH 7.5) under mild agitation condition for 1 hour. Finally, the resulting surfaces were washed 10 times by IDTE buffer (pH 7.5) and were ready to use.

3.3.4 Microfluidic Device Fabrication and Device Performance

PDMS device microfabrication was carried out using a standard soft lithography procedure, as previously described elsewhere [32]. Briefly, a SU-8 master for PDMS microchannels was first prepared by coating a 4-inch silicon wafer with a layer of SU-8 (19 µm in thickness), which was subsequently patterned with straight microchannels using photolithography. Next, ten portions of Sylgard 184 and one portion of curing agent were well mixed before being poured onto the SU-8 master obtained in the previous step. The PDMS mixture was degassed in a vacuum oven for 45 min at room temperature, further crosslinked at 100 ^{o}C for 2h, and finally the cured PDMS microchannel slide was peeled off from the mold. To seal the PDMS microchannel, a cleaned glass slide was used. Briefly, both PDMS microchannel slide and glass slide surfaces were oxygen plasma treated with in a plasma cleaner

(SP100, Anatech Ltd, Battle Creek, MI) at 100 mTorr, 118 W for 10 s, after which the two treated surfaces were immediately bonded together under 1.6 × 10^{-2} MPa pressure at 95 ^{o}C for 30 minutes. Subsequently, stainless steel tubes were inserted at terminals of the microchannels and secured following a protocol as reported elsewhere [179]. Subsequently, the obtained microchannel was surface modified, in sequence, with APTMS, PAMAM and aptamers using the same methodologies as mentioned above, respectively. Finally, the whole microchannel device was ready to use, and its microchannel had a dimension of 20 μm (height) × 90 μm (width) × 4.9 cm (length).

To evaluate the efficacy of the pathogenic bacteria detection performance of the modified microchannels, fluorescent FITC labelled heat killed *E.coli O157:H7* bacteria (annotated *E.coli*-FITC hereinafter) were used as model target bacteria for detection. Specifically, 1 ml *E.coli*-FITC solution (pH 7.5) with variable cell concentrations (ranging from 1×10^2 to 1×10^7 cells/ml) was injected into the microchannels using a syringe pump (Harvard Apparatus, Holliston, MA) at a rate of 0.1 ml/hour. This was followed by a washing step in which the microchannels were washed by air bubbles and nuclease free water several times in order to remove unbound *E.coli*-FITC cells. This preparation allowed the results to be detected and documented by a fluorescence microscope (Olympus IX81, Richmond Hill, ON).

3.4 Numerical Simulation of Staggered Herringbone Microchannels (SHMs)

3.4.1 Design of Staggered Herringbone Microchannels

For the SHMs structures, L-Edit (Version 8.30, Tanner EDA, Monrovia, CA) software was used to create a designed SHM image, which was subsequently imported into COMSOL Multiphysics (Version 4.3b, Burlington, MA) in order to create a 3D structure. As shown in Figure 8, the SHMs consist of two parts, namely microchannels and grooved structures. The microchannel cross-section was of 36 μm (height) × 90 μm (width) dimensions, while the herringbone grooves that were engraved into the slides measured 13.5 μm (depth) × 22.5 μm (width). A full cycle consisted of 12 grooves, the width for all grooves was 22.5 μm, and the gap between two grooves was 22.5 μm.

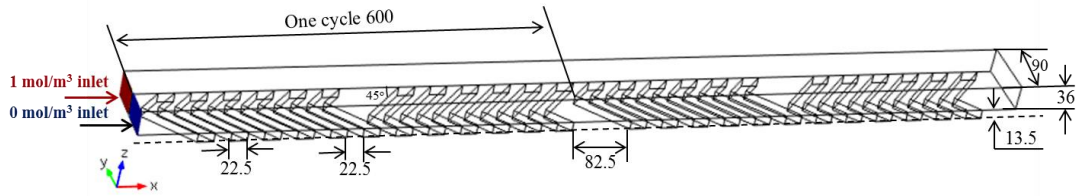

Figure 8. Structure of the simulated SHM (unit in microns).

3.4.2 Transport of Diluted Species Simulation (TDSS)

A Finite Element analysis was used in COMSOL simulation. A free tetrahedral meshing method, with a maximum element size of 5 μm, minimum element size of 0.943 μm, maximum element growth rate of 1.13, resolution of curvature of 0.5, and resolution of narrow regions of 0.8 was used in the TDSS. The simulation was performed via two physical models, i.e. laminar flow model and transport of diluted

species model, and boundary conditions were set based on a previous published study [180]. Specifically, the outlet pressure was set to 0 Pa. In addition, the wall condition was set to "no slip". Fluid concentrations at two inlets were set to 1 mol/m^3 (colored in red) and 0 mol/m^3 (colored in blue), respectively (see Fig 8). Both fluids had the same density at 1×10^3 kg/m^3 and viscosity at 1×10^{-3} $N\ s/m^2$ viscosity), diffusion coefficient was 1×10^{-10} m^2/s, and inlet linear flow rates of velocity of 0.01 m/s were used in both inlets.

3.4.3 Particle Tracing for Fluid Flow Simulation (PTFFS)

The aim of performing PTFFS is to calculate likelihood of particle absorption on the inner wall of this simulated microchannel, as a direct indicator of its operational efficiency. In line with the TDSS simulation, once again two physical models, laminar flow model and particle tracing for fluid flow model, were involved in this simulation. More specifically, the laminar flow model was employed at a stationary stage in Study 1 and incorporated boundary settings. Once again, water served as the liquid flown into the channel, and "no slip" wall condition was adopted. More specifically, a normal inflow velocity of 10 ml/hour was chosen and the outlet pressure was maintained at 0 Pa, as in the TDSS simulation. In the second physical model—particle tracing model—we chose "stick" as the wall condition, in order to simulate the particles sticking onto the channel walls. Thus, once the particles touched the microchannel surface, their movement would cease, and their velocity would be 0 m/s. In addition, we controlled particle density, maintaining it at 2200

kg/m^3, while particle diameter was set to 1×10^{-7} m. Moreover, the drag force was set to obey the Stokes law and "spf/fp1" was selected for both velocity and dynamic viscosity (this check box was chosen during the entire simulation). During the simulation, 100 particles were simultaneously released at the inlets, allowing the proportional density to be typed into the spf.U. This ensured that a greater fluid velocity would result in higher particle density distribution. Finally, freeze condition was chosen from the available outlet options. The entire set of the particle tracing mode settings was computed in a time dependent study (Study 2), which commenced once the results of Study 1 were fully calculated. This sequential processing was necessary, as the solutions used in study 2 were the output of study 1. Before determining the settings, a free tetrahedral mesh was created by calibrating the mesh size to extra fine at fluid dynamics level. This step was required for all grooved structures, while the remaining elements could be predefined as normal, at fluid dynamics level.

Chapter 4. Results and Discussion

4.1 PDMS Surface Modification and Characterization Part

4.1.1 Surface Amination

a. FTIR for Characterization of Surface Amination

In this step, as shown in Figure 9a, three samples were tested by FTIR in order to ensure that $-NH_2$ functional group could be detected on the surface of the PDMS

slides that have been treated by APTMS. The FTIR spectrum of the PDMS surface (after PLAMSA) treated by APTMS was markedly different from that pertaining to the bare PDMS surface. More specifically, the spectrum corresponding to the modified surface was characterized by four peaks at 3343, 1623, 1190 and 883 (cm^{-1}), which were respectively caused by N–H stretching (3500-3300 cm^{-1}), N–H bending (1650-1580 cm^{-1}), C–N stretching (1250–1020 cm^{-1}) and N–H wagging (910-665 cm^{-1}). In addition, C-H stretching (2926±10 cm^{-1}) and C-H sym stretching (2853±10 cm^{-1}) contributed to the $–CH_2–$ group peaks at 2920 cm^{-1} and 2846 cm^{-1}, respectively [181-183]. Thus, it can be postulated that these peaks are caused by the amino and hydrocarbon functional group introduced by conjugating APTMS. However, the sample treated by APTMS without prior plasma processing produced an identical FTIR spectrum to that pertaining to bare PDMS, indicating that the APTMS cannot be conjugated on the PDMS surface without plasma treatment.

b. Surface Amino Quantification

Fluorescence labeling is a very useful method, as it allows identification of parameters that affect the level of amination on PDMS surfaces [32, 176-178]. As shown in Figure 9b, greater fluorescence intensities were obtained at higher APTMS concentrations, with the greatest intensity obtained for the last group. However, in the last group, amino groups could not be evenly distributed throughout the PDMS surface. Hence, higher APTMS concentration could easily form insoluble particles when the surfaces are exposed to the air. This phenomenon occurs because APTMS

is capable of self-condensation, whereby it forms gel when in contact with water molecules [184]. When compared to other groups, APTMS (5 wt %) that was incubated for 20 seconds, and rhodamine-NHS incubated for 30 minutes were selected as the implementation condition, because this group has relatively higher fluorescent intensity and resulted in much more uniform performance on the surface of PDMS.

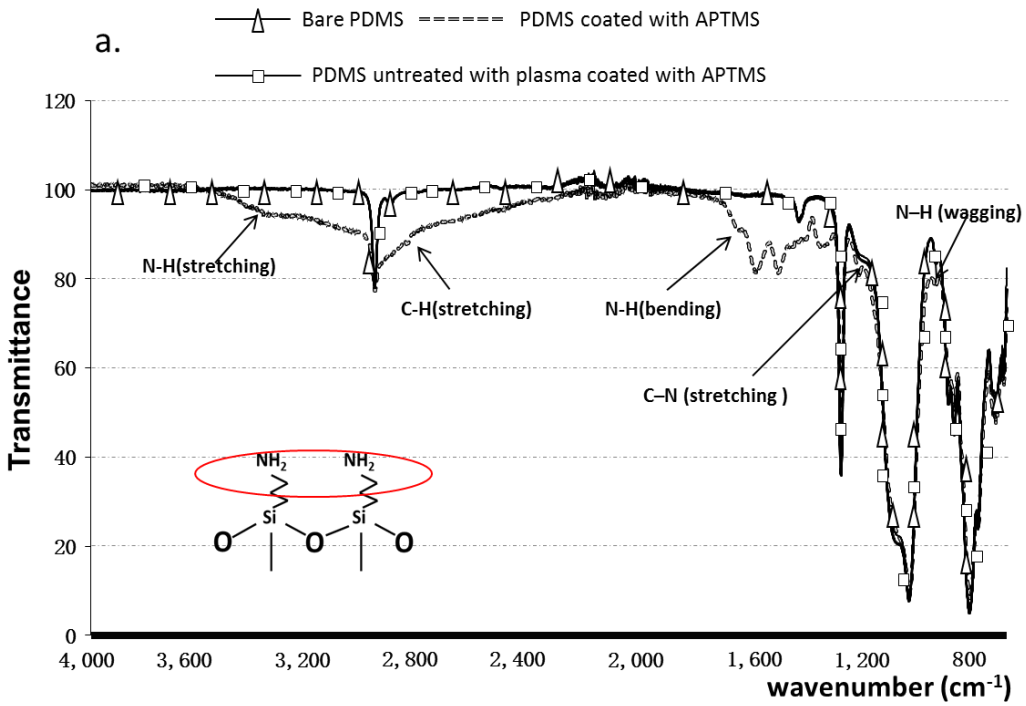

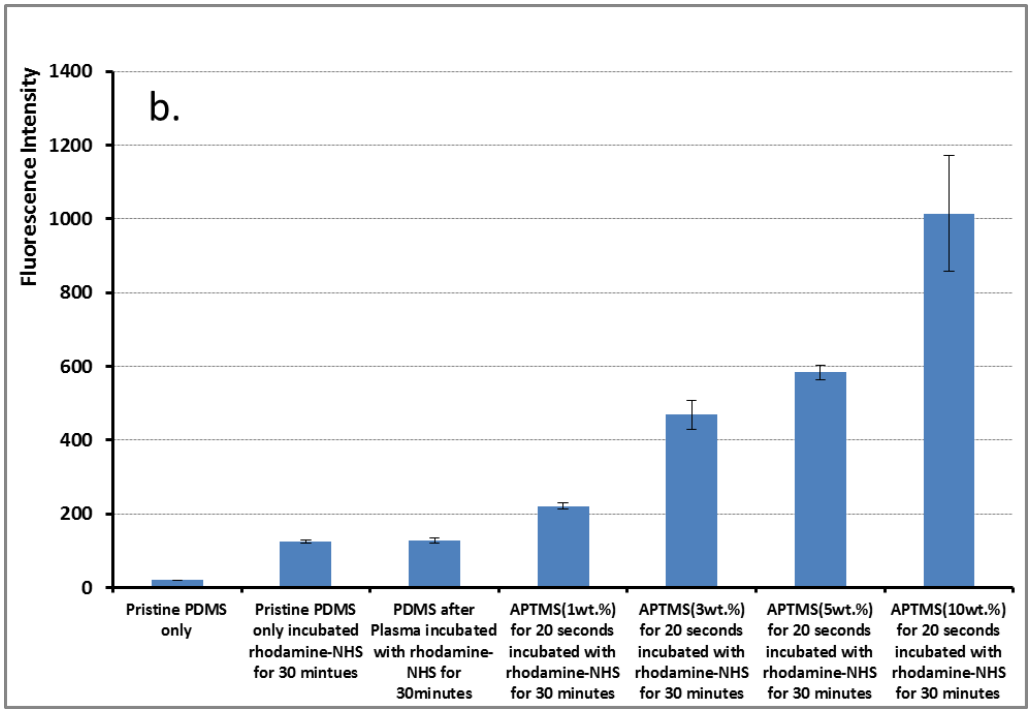

Figure 9. PDMS surface amination. a. FTIR test for $-NH_2$ bound after surface treated by APTMS. b. Relative fluorescence intensities of PDMS surfaces aminated under different conditions. Error bars indicate the standard deviation of seven measured relative fluorescence intensities on each sample surface.

4.1.2 PAMAM Engraftment

a. PAMAM Surface Quantification

In this study, PAMAM-NHS was used as a fluorescent label marker for PAMAM conjugated onto APTMS-modified PDMS surface through an amine/carboxyl reaction. The aim of this experiment was to identify the most optimal reaction conditions when the PAMAM molecules were grafted on the target surfaces. In order to achieve these objectives, three steps were performed, whereby one of the three conditions was changed sequentially, while the remaining two remained fixed. Thus,

the process involved assessing the effects of modifying plasma activation time, APTMS incubation time and PAMAM concentration.

More specifically, when APTMS incubation time was set to 20 seconds, the highest fluorescence intensity was obtained, as no other reaction time produced similar effect. This result is most likely due to shorter incubation time (10 s) being insufficient for the APTMS molecules to fully react with hydroxyl groups on the surface. On the other hand, longer incubation time (40 s) was likely to result in APTMS self-condensation, which would hydrolyze forming insoluble layer, blocking fluorescence intensity [184]. Moreover, when the effect of plasma activation time on fluorescence intensity was tested, the findings indicated that the activation time of 10 seconds produced the highest fluorescence intensity. Thus, we posit that this phenomenon arises because shorter plasma activation period (5 s) would not full change the surface structure into hydroxyl functional groups, while longer plasma activation time (30 s) would cause the PDMS surface to crack. As a result, an extremely brittle silica layer would form on the surface [79, 185], which will affect the APTMS conjugation. Finally, when PAMAM concentrations were changed, while keeping the remaining two parameters constant, the resulting fluorescence intensities increased at greater PAMAM concentrations, suggesting that higher bulk PAMAM concentration contributes to higher APTMS conjugation on an amino-pretreated surface. Therefore, PAMAM concentration at 4.0 μM was selected as the optimum condition. (Figure in Appendices A2)

b. PAMAM Surface Characterization

To characterize the success of the PAMAM immbolization on PDMS surface, water contact angle (WCA), XPS and AFM were used to test the hydrophobicity, morphology and chemical element composition of the PAMAM-immobilized surfaces. As shown in Figure 10a, the bare PDMS surface was successfully modified by PAMAM-COOH via pretreated plasma and amination, due to corresponding changes in WCA [181, 186]. It is also worthy to note the AFM images in Fig. 10b, which reveal that PDMS surfaces become rougher after PAMAM immobilization. On the other hand, the surface structure of the PDMS surfaces treated with APTMS did not change significantly. Lastly, in Fig. 10c, significant changes in the chemical composition can be seen after PAMAM is enriched on the PDMS surface. The data used to produce these images were analyzed and processed according to the protocols reported in previously published work [187]. It is also noteworthy that, before and after surface modification, the peaks corresponding to N 1S and C 1S exhibited dramatic differences, indicating that C-N [188], (C=O)-NH [188], C=O [187],C-H(C) [189] and (C=O)-O [190] chemical structures emerged after modification. Moreover, the fact that C-H and C-Si structures (C 1s) are no longer present after PAMAM immobilization further confirms that coated materials affected the PDMS surface [191]. Thus, we can posit that these characterization methods yielded results that serve as strong evidence of PAMAM being successfully grafted onto the PDMS surface.

a.

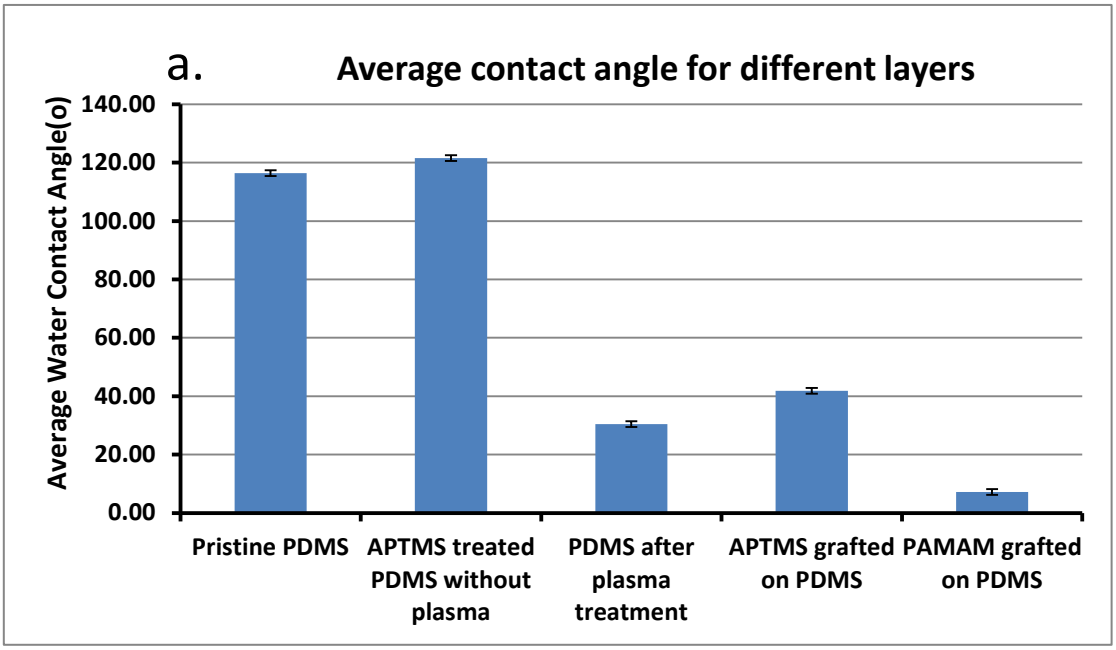

b.

PDMS samples	Pristine PDMS	PDMS with APTMS	PAMAM on PDMS
AFM 3D Images	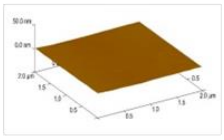	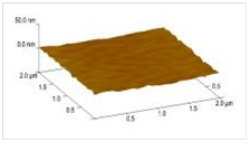	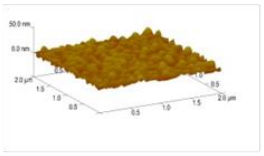
AFM Plane Form	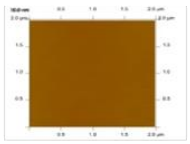	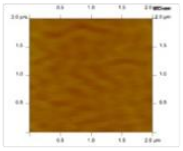	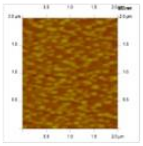
Roughness（nm）	0.412±0.02	1.20±0.07	4.52±0.31

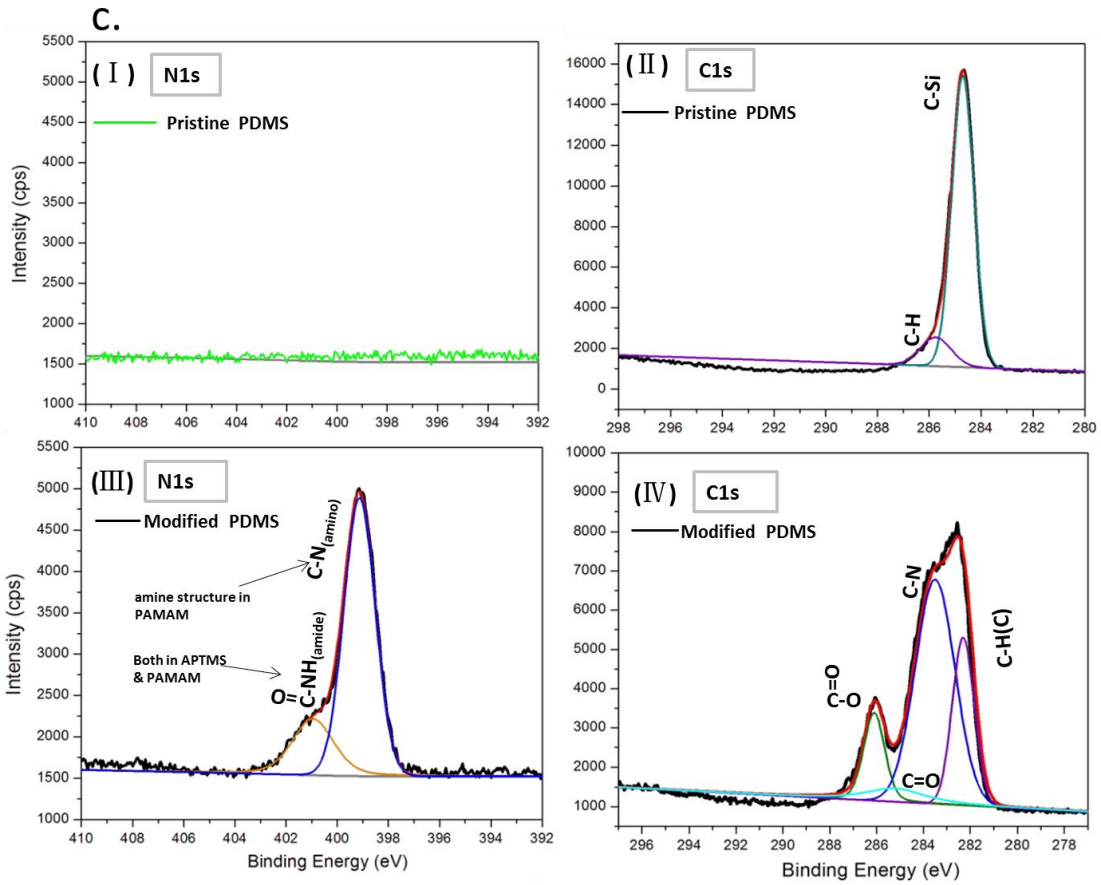

Figure 10. PAMAM surface characterization. a. WCA measurement of PAMAM surface coated with different chemicals. b. The 3D topology pictures of PDMS surfaces include two control surfaces. c. High resolution XPS spectra of unmodified and modified surfaces; i, N1S pristine PDMS surface. ii, C1S pristine PDMS surface. iii, N1S PAMAM modified PDMS surface. iv, C1S PAMAM modified PDMS surface.

4.1.3 Aptamers Engraftment

a. Quantification of Aptmaers Engraftment

In order to investigate aptamer engraftment, we tested average fluorescence intensity of the PDMS surface under different conditions, aiming to identify the most optimal experiential conditions for aptamer conjugation. In the experiment whose findings are shown in Figure 11, a pristine PDMS surface was used as the control

group. As can be seen, the second (without amination) and the third (no PAMAM immobilization) groups were characterized by relatively higher fluorescence intensity than that obtained from the control group, most likely because of the nonspecific absorption of Cy3-aptamers on the surfaces. However, the fourth group (no NHS/EDC) and the last group showed a generally increasing trend in fluorescence intensity. Finally, the highest fluorescence intensity was associated with the group comprising of G7-PAMAM incubated in Cy3-aptamers activated by NHS/EDC. We posit that this phenomenon is due to the ability of NHS/EDC to promote the reaction process in this group. Consequently, the last group was used as the optimum condition in this study.

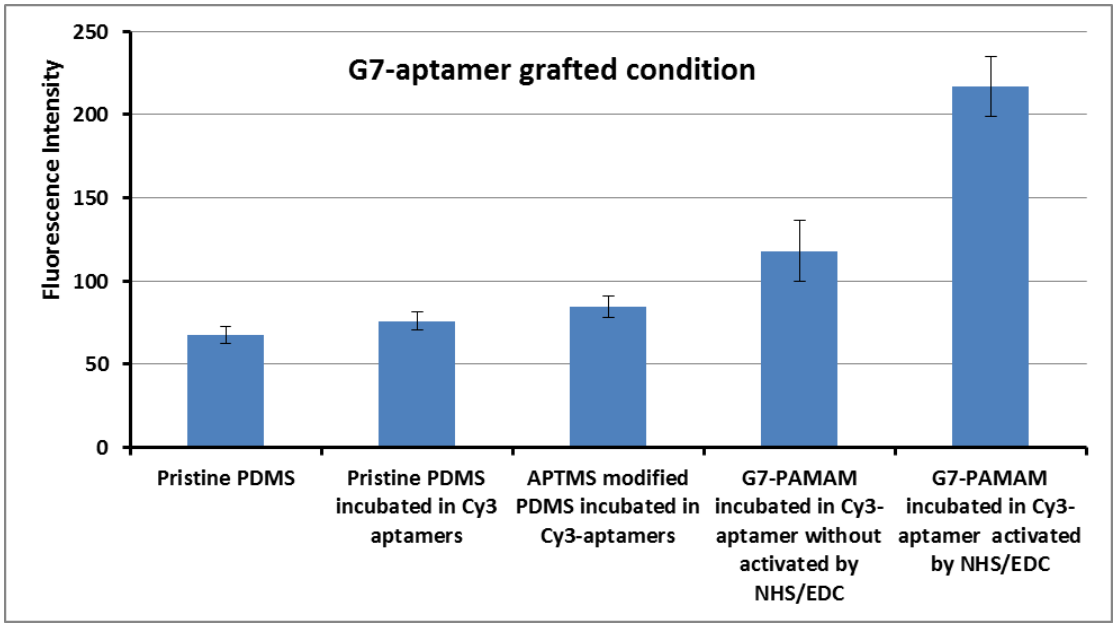

Figure 11. Fluorescence intensity of PDMS surfaces under cy3-aptamers engraftment under different conditions. Error bars indicate the standard deviation of eight measured relative fluorescence intensities on each sample surface.

4.2 Escherichia coli O157:H7 Detection Part

4.2.1 Device Performance

In order to assess the device performance, FITC-labeled *E.coli O157:H7* was injected into different modified channels (at 0.1 ml/hr), (a) Blank channels, (b) G7 only channels, (c) G4 only channels, (d) G7 disarray-aptamer channels, (e) G4 disarray-aptamer channels, (f) G7 aptamer channels, and (g) G4 aptamer channels, at a various cell concentrations (ranging from 10^7 to 10^2 cell/ml). These channels were subsequently washed before being observed under the fluorescent microscope, with the resulting images shown in Figure 12. As can be seen, in blank channels, owning to nonspecific PDMS absorption, only a few *E.coli* attached onto the channel surface, even when *E.coli* were present at very high concentrations (10^7 to 10^6 cell/ml). Compared with the image shown in panel (a), in image (b) no *E.coli* appears to be attached onto the G7 modified surface. This finding can be explained by the fact that PAMAM chain has higher extension and flexibility [32, 81, 192], and this chain structure could cause strong steric interactions, which can block the attractive interactions between *E.coli* and PDMS channel surface to prevent nonspecific absorption [32, 192]. The images pertaining to G7 and G4 disarray-aptamer channels (image d and e) reveal that, when the concentration reaches and exceeds 10^6 cells/ml, only a few *E.coli* can adhere onto the channel surface. In addition, no specific adherence pattern can be observed, most likely because of the weak electronegativity of DNA molecules. However, images (f) and (g) show that *E.coli*

could be specifically captured by aptamer-modified microchannels. This is likely due to the correct choice of DNA oligos, which are characterized by specific binding with *E.coli*, unlike disarray aptamers in image (d) and (e). It should be noted that the difference in performance observed in images (f) and (g) can be interpreted as the limit of detection (LOD) of our device. We further posit that the LOD of G7 aptamer channels could be as low as 10^2 cells/ml, while that of G4 aptamer channels is slightly higher at 10^3 cell/ml.

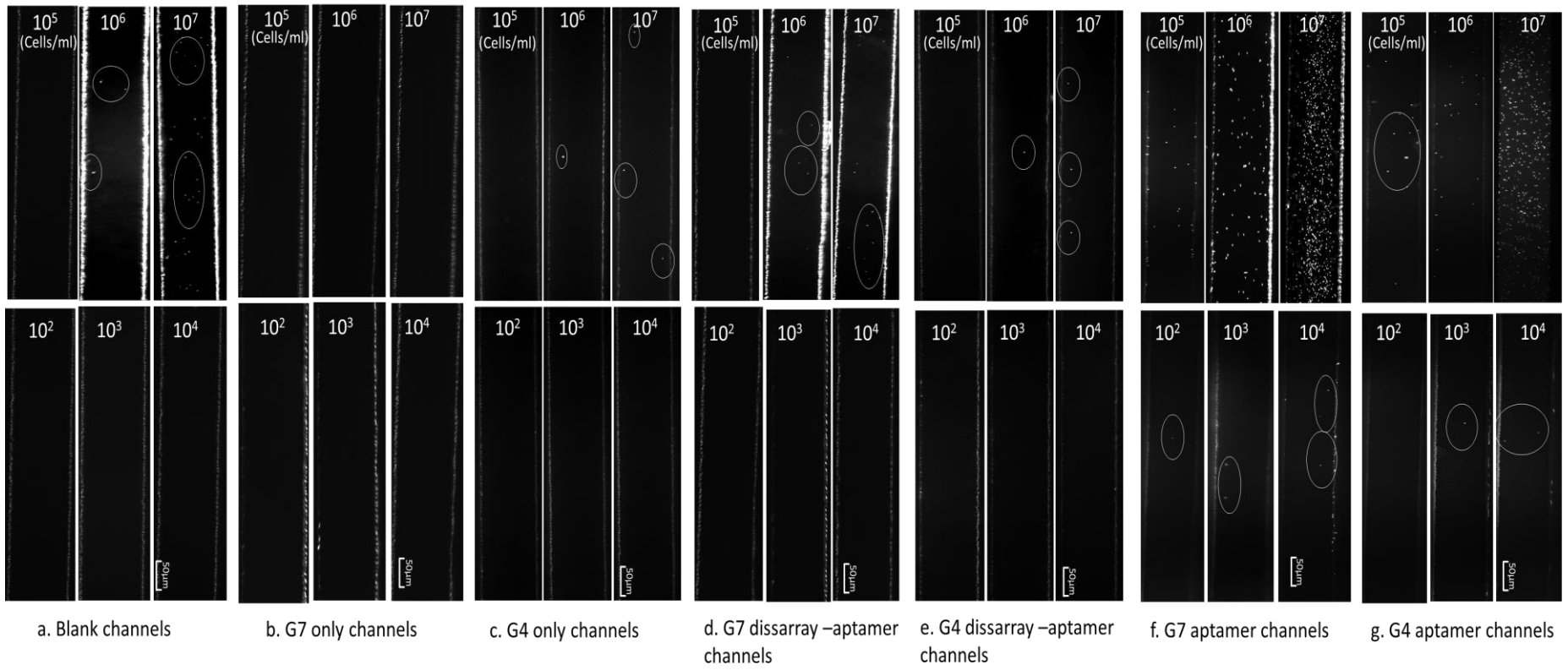

Figure 12. Microchannel performances at different injected *E.coli* concentrations. (a) Blank channels, (b) G7 only channels, (c) G4 only channels,(d) G7 disarray-aptamer channels , (e) G4 disarray-aptamer channels, (f) G7 aptamers channels, (g) G4 aptamers channels

In a further step, in order to demonstrate that G7 aptamer-modified channels could improve the LOD, we counted the number of captured *E.coli* in both G4 and G7 aptamer-modified channels. The obtained results were subsequently plotted, revealing an interesting pattern between the two modified microchannels. Figure 13a shows G4 aptamer channel performance vs. G7 aptamer channel performance with respect to the ability to capture *E.coli*. When the cell concentration reaches 10^5 cell/ml, the number of captured *E.coli* in G4 aptamer channel corresponds to 57% of that obtained in the G7 aptamer channel. However, this percentage declined to 41% and 15%, respectively, as the cell concentration declined from the original 10^5 cells/ml to 10^4 cells/ml and 10^3 cells/ml. It is, however, noteworthy that, when the cell concentration decreased to 100 cell/ml, G4 could not detect any *E.coli*. The reason behind this observation lies in the LOD of the G4 aptamer-modified microchannel that, at 10^3 cell/ml, cannot capture any *E.coli* at these low concentrations. In contrast, at 100 cells/ml concentration, there are still several *E.coli* captured in the G7 aptamer channel (Figure 12f), as the LOD of the G7 aptamer-modified channels is 10^2 cell/ml, which is also lower than the LOD reported in most previous studies [21, 22, 25, 34]. Overall, these findings indicate that, at a very low *E.coli* concentration stage, G7 aptamer channels outperform both G4 aptamer channels and other modified channels tested in this work. This superior performance most likely results from the presence of relatively more “branched” structure on G7 molecules, relative to G4, which could increase the likelihood of *E.coli* conjugating with aptamers engrafted on these “branches”. In sum, the

branch-like structure of PAMAM (G7) could improve the microchannel detection ability when employed for the purpose of *E.coli* inspection. Moreover, the LOD could be decreased by increasing the prevalence of these “branches” on dendrimers in both G4 and G7 structures.

We also compared the relative quantity of aptamer conjugation conditions between G4- and G7-modified PDMS surfaces. The same G4 and G7 concentrations were used in this experiment, and the surfaces were processed in the manner described in the previous case. Moreover, the same method was used for calculating fluorescence intensity. Figure 13b pertains to PAMAM-G4 PDMS surface and PAMAM-G7 PDMS surface groups, where it can be seen that their fluorescence intensity remained virtually unchanged. This finding implies that the nonspecific absorption of Cy3-aptamer on the PDMS surface could be negligible. However, when G4-Aptamer-Cy3 grafted surface and G7-Aptamer-Cy3 grafted surface groups were examined, the fluorescence intensity produced exhibited a dramatic increase in the peaks at 104 and 236 cm^{-1} respectively, which suggests that the capacity of aptamers on the G7 modified surface could be almost two times higher than that on the G4 conjugated PDMS surface. Theoretically, the capacity of G7 molecules to combine with aptamer molecules could be eight times higher than the capacity of G4 polymers, as the number of primary carboxyl functional groups on every PAMAM molecules is 64 (G4) and 512 (G7), respectively [114] (each carboxyl group will link with an aptamer). However, in experiential conditions, PAMAM molecules could not be evenly engrafted onto the PDSM surface, and the fluorescence could also be

affected by the environment. Thus, we can confirm that, compared to the G4 modified surfaces, the G7 modified surfaces have a higher capacity for conjugating aptamers.

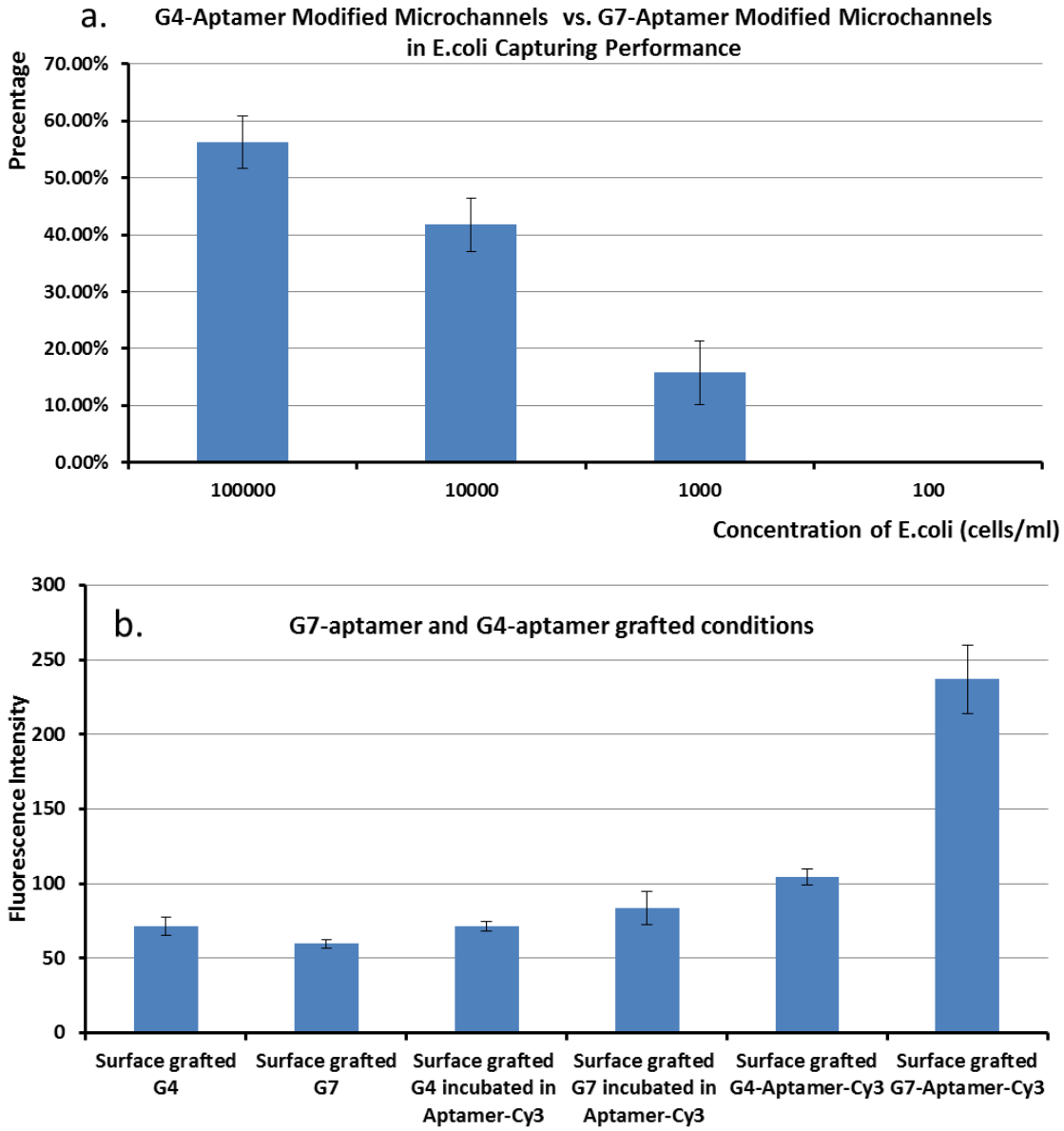

Figure 13. a. G4-Aptamer modified microchannels vs. G7-Aptamer modified microchannels in *E.coli* capturing performance b. Fluorescence intensity of G4 and G7 modified PDMS surfaces under cy3-aptamers engraftment. Error bars indicate the standard deviation of relative fluorescence intensities on each sample surface.

4.3 Numerical Simulation Part

Low Reynolds (Re = 0.64) number flow condition of straight microchannels used for detection will affect the possibility that *E.coli* will be conjugated with the immobilized aptamers. This limitation arises because, at the low Re stage, pressure flows in straight channels are laminar and uniaxial, and diffusive mixing is negligible [193]. Therefore, it would be difficult for the *E.coli* in the middle of the microchannels to reach the microchannel surfaces. Consequently, microchannel efficiently would be substantially reduced under this condition. Hence the SHMs have been simulated to assess the ability of this channel structure to overcome this limitation.

4.3.1 Transport of Diluted Species Simulation (TDSS)

In TDSS, we simulated mixing of two fluids within microchannels. In the simulation, two fluids with different concentrations were marked with red (1 mol/m^3) and blue colors (0 mol/m^3), and 19 cross-sectional concentration profiles were chosen along the length of two different microchannels, namely an SHM (large images on the left) and a straight microchannel (small images shown in the right corner). In Figure 14a, the SHM is believed to mix in a dynamic manner along the channel length because, at the beginning (0 μm), the red and blue color can be clearly distinguished. However, as the microchannel length increases, the color mixing occurs, and light blue color appears. This indicates that the two concentrations are intermediate, as the two fluids are fully mixed at the end of the

microchannel (at 5980 μm). In contrast, the concentrations in the straight channel remained almost unchanged, because flows in straight microchannels are laminar and uniaxial. This indicates that using the SHM configuration would improve dynamic of micromixing process and increase the likelihood of *E.coli* attaching to the surface of microchannels.

4.3.2 Particle Tracing for Fluid Flow Simulation (PTFFS)

In PTFFS, when the simulated particles touched the microchannel surfaces, the tracing objects would be frozen. Thus, this simulation could reflect a real experimental situation. Drawing upon this theory, the particle absorption conditions of an SHM and a normal channel were simulated simultaneously, and nine length points were selected to calculate their absorption possibilities. As can be seen in Figure 14b, the percentage of particles absorbed on both microchannels exhibited a linear upward trend. However, the increase in the particle absorption rate of grooved microchannels is much greater than that of the straight channels. In particular, at the beginning (2550 μm), the particle absorption probability of grooved channels is 7% (100 particles released at the same time). Nonetheless, no particle was absorbed on the straight microchannel surface at this length, and even at the end of the channel length (11000 μm), the grooved channels could absorb 81% particles, whereas the straight channels achieved only 5% absorption.

Thus, according to the tendency we observed in this work, we can predict that, when microchannel length reaches 12000 μm, the particle absorption percentage

could be as high as 90%, or even be exceeded in grooved channels. Moreover, when we compared the simulated data pertaining to straight microchannels with the experimental results (in Figure 12f, with 10^2 and 10^3 cell concentrations) obtained for the same channel length (11000 μm), using the maximum computer processing power, we found very similar cell-capture probabilities. More specifically, about 5% was obtained in simulations, while approximately 5% and 4% was yielded by the experiments, corresponding to 10^2 and 10^3 cell concentrations, respectively. The relatively higher likelihood of cell capture in the simulation was attributed the special boundary conditions, where the particles were treated as captured immediately after touching the wall. In contrast, in the experimental conditions, this was not the case, thus leading to lower capture percentage. Therefore, these data could serve as evidence that the SHM could improve the work efficiency of microchannels.

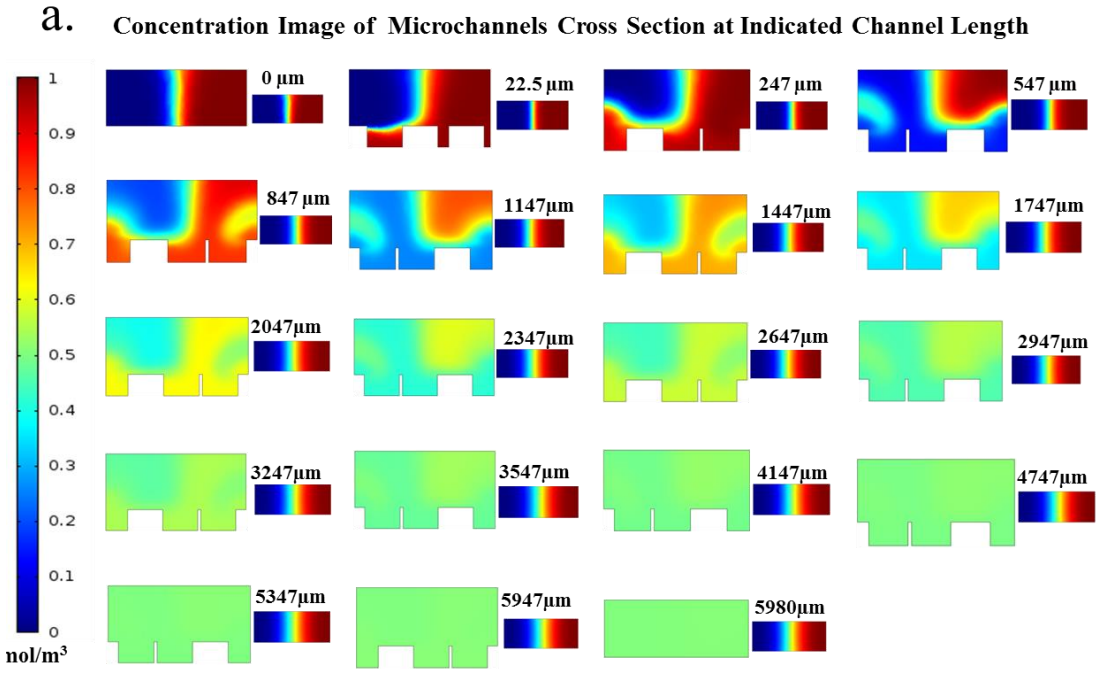

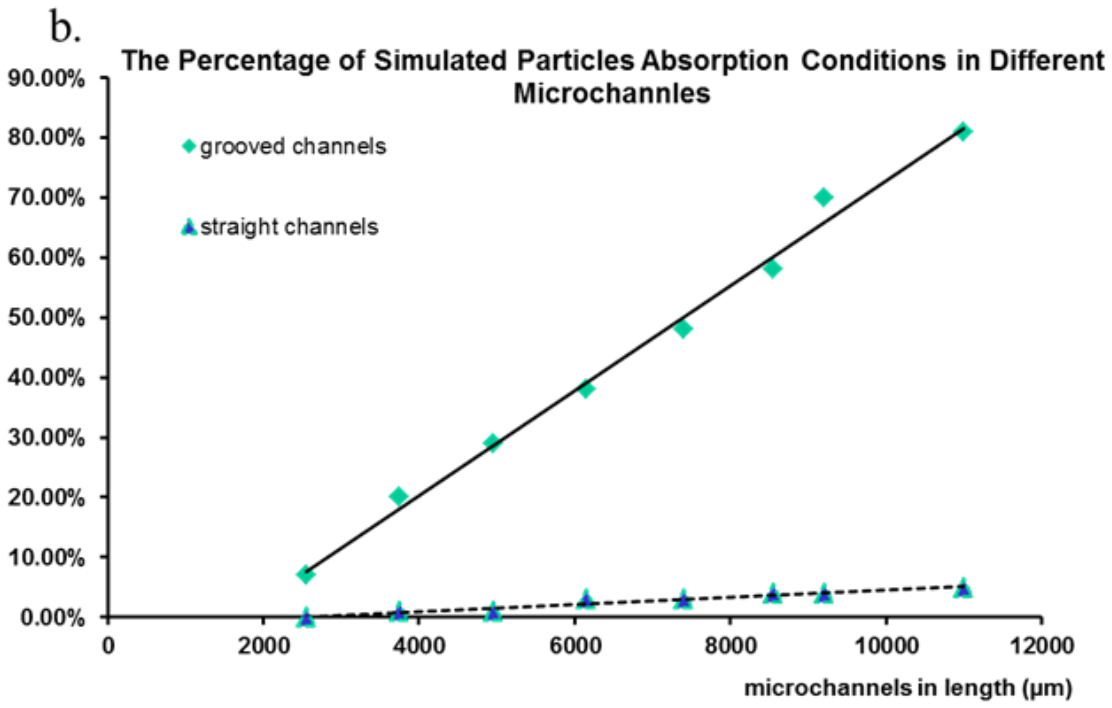

Figure 14. Numerical simulation of SHM in two different modules. a. Concentration image of the channel cross section at indicated channel length; large images of the left are the SHM and small images of the right corner are the straight channel. b. The percentage of simulated particles absorption conditions in different microchannels.

Chapter 5. Conclusions

In this study, we examined two layer modification methods by introducing dendrimers and aptamers onto the surface of PDMS-based microfluidic system aiming to improve the sensitivity of *Escherichia coli O157:H7* detection. In addition, we simulated staggered herringbone microchannels (SHMs) by using Comsol software to evaluate the work efficiency of SHMs when employed in *E.coli* detection. The results reported here show that the LOD of our device with respect to sensitivity to *Escherichia coli O157:H7* is 10^2 cells/ml, which is lower than that reported in previous works [21, 22, 25, 34]. We further demonstrate that the SHMs can

significantly improve the particle absorption conditions on the microchannel surface. In the microchannel layer modification phase of our study, we found that the plasma activation and APTMS concentration are the main factors affecting the level of PAMAM-COOH conjugation, which consequently influences the level of aptamers that have affinity to *Escherichia coli O157:H7*. Moreover, we have also demonstrated that dendrimers have non-fouling function and can thus prevent particles from attaching to the channel surfaces. Finally, the LOD of the G7 aptamer-modified microchannel is lower than that of the G4 aptamer-modified microchannel. Our simulation results revealed that, as the length of microchannels increases, the grooved channels are more favorable, as this geometry increases the particle capture rate. In future studies, it would be useful to design and test rolling cycle amplification test for *E.coli*. This setup can be incorporated in to this system for signal enhancement. In addition, we plan to test other organisms in the modified microfluidic devices, thus increasing the application scope of our work.

Chapter 6. Future Work

In this work, it was shown that *E.coli*. can be successfully detected by dendrimer-aptamer modified microchannels in a level of 10^2 cells/ml with 10 hours. Because our present work is based on detection stage, in order to achieve a better detection performance and a shorter detection time, it would be interesting to conduct the following experiments:

1. To study a better isolation method for *E.coli* sample from a real-word food sample. Comparing with plate culture method, the new method should have a several advantages: 1. Bacterial could be separated from the real-word food sample directly without have cell enrichment process. 2. Methods should purify the bacterial solution to filter large particles which have potentials to block microfluidic system. 3. The separation should be better limited in several hours.
2. To design and test rolling cycle amplification for E.coil test signal enhancement. Our present work uses preprocessed fluorescence labeled *E.coli*. as a detection object, so when we apply bacterial from a real-world food sample in this system, we need use rolling cycle amplification method to increase the detection signal.
3. To manufacture grooved channels with different geometry. To get a better mixing condition inside of the microfluidic channels, produce different size of micromixer is indispensable.
4. To design new readout format for detection signals. At present stage of this project, the readout format is manually counted the number of *E.coli*. captured by microchannels, which is quite labor-intensive and time-consuming. Therefore, new readout format should be automatic and time-efficient.
5. To prove the specific detection of *E.coli* aptamers by comparing with results that from other organisms. We should use other non-*E.coli. O157: H7* strains

into the present microfluidic system to confirm that the aptamers are only specific for *E.coli. O157: H7.*

References

1. Hancock, D.D., et al., *Multiple sources of< i> Escherichia coli</i> O157 in feedlots and dairy farms in the Northwestern USA.* Preventive veterinary medicine, 1998. **35**(1): p. 11-19.
2. Mead, P.S. and P.M. Griffin, *< i> Escherichia coli</i> O157: H7.* The Lancet, 1998. **352**(9135): p. 1207-1212.
3. Johnsen, G., et al., *< i> Escherichia coli</i> O157: H7 in faeces from cattle, sheep and pigs in the southwest part of Norway during 1998 and 1999.* International journal of food microbiology, 2001. **65**(3): p. 193-200.
4. Willshaw, G., et al., *Verocytotoxin-producing Escherichia coli (VTEC) O157 and other VTEC from human infections in England and Wales: 1995–1998.* Journal of medical microbiology, 2001. **50**(2): p. 135-142.
5. Canada food inspection agency. *http://www.inspection.gc.ca/about-the-cfia/newsroom/food-recall-warnings/complete-listing/2014-07-21/eng/1405996324343/1405996325358*. 2014 2014/07/21 [cited 2015/03/15 2015/03/15].
6. Lazcka, O., F. Campo, and F.X. Munoz, *Pathogen detection: A perspective of traditional methods and biosensors.* Biosensors and Bioelectronics, 2007. **22**(7): p. 1205-1217.
7. Chang, C.-M., et al., *Nucleic acid amplification using microfluidic systems.* Lab on a Chip, 2013. **13**(7): p. 1225-1242.
8. Niemeyer, C.M., R. Wacker, and M. Adler, *Combination of DNA-directed immobilization and immuno-PCR: very sensitive antigen detection by means of self-assembled DNA–protein conjugates.* Nucleic acids research, 2003. **31**(16): p. e90-e90.
9. Anderson, R.C., et al., *A miniature integrated device for automated multistep genetic assays.* Nucleic Acids Research, 2000. **28**(12): p. e60-e60.
10. Blais, B., et al., *Comparison of fluorogenic and chromogenic assay systems in the detection of Escherichia coli O157 by a novel polymyxin-based ELISA.* Letters in applied microbiology, 2004. **39**(6): p. 516-522.
11. Magliulo, M., et al., *A rapid multiplexed chemiluminescent immunoassay for the detection of*

Escherichia coli O157: H7, Yersinia enterocolitica, Salmonella typhimurium, and Listeria monocytogenes pathogen bacteria. Journal of agricultural and food chemistry, 2007. **55**(13): p. 4933-4939.

12. Haque, R., et al., *Diagnosis of pathogenic Entamoeba histolytica infection using a stool ELISA based on monoclonal antibodies to the galactose-specific adhesin.* Journal of Infectious Diseases, 1993. **167**(1): p. 247-249.
13. Schumacher, J., J.W. Randles, and D. Riesner, *A two-dimensional electrophoretic technique for the detection of circular viroids and virusoids.* Analytical biochemistry, 1983. **135**(2): p. 288-295.
14. Beyor, N., et al., *Integrated capture, concentration, polymerase chain reaction, and capillary electrophoretic analysis of pathogens on a chip.* Analytical chemistry, 2009. **81**(9): p. 3523-3528.
15. Zharov, V.P., et al., *Photoacoustic flow cytometry: principle and application for real-time detection of circulating single nanoparticles, pathogens, and contrast dyes in vivo.* Journal of biomedical optics, 2007. **12**(5): p. 051503-051503-14.
16. Hahn, M.A., P.C. Keng, and T.D. Krauss, *Flow cytometric analysis to detect pathogens in bacterial cell mixtures using semiconductor quantum dots.* Analytical chemistry, 2008. **80**(3): p. 864-872.
17. Tilden Jr, J., et al., *A new route of transmission for Escherichia coli: infection from dry fermented salami.* American Journal of Public Health, 1996. **86**(8_Pt_1): p. 1142-1145.
18. Rivas, L., et al., *Detection and Typing Strategies for Pathogenic Escherichia coli*. 2015: Springer.
19. Swensen, J.S., et al., *Continuous, real-time monitoring of cocaine in undiluted blood serum via a microfluidic, electrochemical aptamer-based sensor.* Journal of the American Chemical Society, 2009. **131**(12): p. 4262-4266.
20. Xu, Y., X. Yang, and E. Wang, *Review: Aptamers in microfluidic chips.* Analytica chimica acta, 2010. **683**(1): p. 12-20.
21. Yoo, J.H., et al., *Microfluidic based biosensing for< i> Escherichia coli</i> detection by embedding antimicrobial peptide-labeled beads.* Sensors and Actuators B: Chemical, 2014. **191**: p. 211-218.

22. Zordan, M.D., et al., *Detection of pathogenic E. coli O157: H7 by a hybrid microfluidic SPR and molecular imaging cytometry device.* Cytometry Part A, 2009. **75**(2): p. 155-162.

23. Baeumner, A.J., et al., *RNA biosensor for the rapid detection of viable< i> Escherichia coli</i> in drinking water.* Biosensors and Bioelectronics, 2003. **18**(4): p. 405-413.

24. Che, Y., Y. Li, and M. Slavik, *Detection of< i> Campylobacter jejuni</i> in poultry samples using an enzyme-linked immunoassay coupled with an enzyme electrode.* Biosensors and Bioelectronics, 2001. **16**(9): p. 791-797.

25. Radke, S.M. and E.C. Alocilja, *A high density microelectrode array biosensor for detection of< i> E. coli</i> O157: H7.* Biosensors and Bioelectronics, 2005. **20**(8): p. 1662-1667.

26. Le Berre, V., et al., *Dendrimeric coating of glass slides for sensitive DNA microarrays analysis.* Nucleic Acids Research, 2003. **31**(16): p. e88-e88.

27. Li, G., et al., *Dendrimers-based DNA biosensors for highly sensitive electrochemical detection of DNA hybridization using reporter probe DNA modified with Au nanoparticles.* Biosensors and Bioelectronics, 2009. **24**(11): p. 3281-3287.

28. Li, Z., et al. *Aptamer-conjugated dendrimer-modified quantum dots for glioblastoma cells imaging*. in *Journal of Physics: Conference Series*. 2009. IOP Publishing.

29. Liu, H., et al., *DNA-templated covalent coupling of G4 PAMAM dendrimers.* Journal of the American Chemical Society, 2010. **132**(51): p. 18054-18056.

30. Astruc, D., E. Boisselier, and C. Ornelas, *Dendrimers designed for functions: from physical, photophysical, and supramolecular properties to applications in sensing, catalysis, molecular electronics, photonics, and nanomedicine.* Chemical Reviews, 2010. **110**(4): p. 1857-1959.

31. Han, H.J., et al., *Multifunctional Dendrimer-Templated Antibody Presentation on Biosensor Surfaces for Improved Biomarker Detection.* Advanced functional materials, 2010. **20**(3): p. 409-421.

32. Yeh, P.Y., et al., *Nonfouling hydrophilic poly (ethylene glycol) engraftment strategy for PDMS/SU-8 heterogeneous microfluidic devices.* Langmuir, 2012. **28**(46): p. 16227-16236.

33. Jayasena, S.D., *Aptamers: an emerging class of molecules that rival antibodies in diagnostics.* Clinical chemistry, 1999. **45**(9): p. 1628-1650.

34. Tims, T.B. and D.V. Lim, *Rapid detection of< i> Bacillus anthracis</i> spores directly from*

powders with an evanescent wave fiber-optic biosensor. Journal of microbiological methods, 2004. **59**(1): p. 127-130.

35. Karch, H., P.I. Tarr, and M. Bielaszewska, *Enterohaemorrhagic< i> Escherichia coli</i> in human medicine.* International Journal of Medical Microbiology, 2005. **295**(6): p. 405-418.
36. wikipedia. *http://en.wikipedia.org/wiki/Escherichia_coli_O157:H7*. 2014 2014/06/07 [cited 2014 June 13].
37. Riley, L.W., et al., *Hemorrhagic colitis associated with a rare Escherichia coli serotype.* New England Journal of Medicine, 1983. **308**(12): p. 681-685.
38. Johnson, W., H. Lior, and G. Bezanson, *Cytotoxic Escherichia coli 0157: H7 associated with haemorrhagic colitis in Canada.* The Lancet, 1983. **321**(8314): p. 76.
39. Belongia, E.A., et al., *An outbreak of Escherichia coli 0157: H7 colitis associated with consumption of precooked meat patties.* Journal of infectious diseases, 1991. **164**(2): p. 338-343.
40. Carter, A.O., et al., *A severe outbreak of Escherichia coli O157: H7–associated hemorrhagic colitis in a nursing home.* New England Journal of Medicine, 1987. **317**(24): p. 1496-1500.
41. Dev, V.J., M. Main, and I. Gould, *Waterborne outbreak of Escherichia coli 0157.* The Lancet, 1991. **337**(8754): p. 1412.
42. Ostroff, S.M., et al., *A STATEWIDE OUTBREAK OF ESCHERICHIA-COLI O157-H7 INFECTIONS IN WASHINGTON-STATE.* American Journal of Epidemiology, 1990. **132**(2): p. 239-247.
43. Pavia, A.T., et al., *HEMOLYTIC-UREMIC SYNDROME DURING AN OUTBREAK OF ESCHERICHIA-COLI O157-H7 INFECTIONS IN INSTITUTIONS FOR MENTALLY-RETARDED PERSONS - CLINICAL AND EPIDEMIOLOGIC OBSERVATIONS.* Journal of Pediatrics, 1990. **116**(4): p. 544-551.
44. Spika, J.S., et al., *HEMOLYTIC UREMIC SYNDROME AND DIARRHEA ASSOCIATED WITH ESCHERICHIA-COLI O157-H7 IN A DAY-CARE-CENTER.* Journal of Pediatrics, 1986. **109**(2): p. 287-291.
45. Ryan, C.A., et al., *ESCHERICHIA-COLI O157-H7 DIARRHEA IN A NURSING-HOME - CLINICAL, EPIDEMIOLOGIC, AND PATHOLOGICAL FINDINGS.* Journal of Infectious Diseases, 1986. **154**(4): p. 631-638.

46. Rowe, P.C., et al., *HEMOLYTIC-ANEMIA AFTER CHILDHOOD ESCHERICHIA-COLI O 157.H7 INFECTION - ARE FEMALES AT INCREASED RISK.* Epidemiology and Infection, 1991. **106**(3): p. 523-530.

47. Rowe, P.C., et al., *EPIDEMIOLOGY OF HEMOLYTIC-UREMIC SYNDROME IN CANADIAN CHILDREN FROM 1986 TO 1988.* Journal of Pediatrics, 1991. **119**(2): p. 218-224.

48. Lior, H., *INCIDENCE OF HEMORRHAGIC COLITIS DUE TO ESCHERICHIA-COLI IN CANADA.* Canadian Medical Association Journal, 1988. **139**(11): p. 1073-1074.

49. Swerdlow, D.L., et al., *A WATERBORNE OUTBREAK IN MISSOURI OF ESCHERICHIA-COLI-O157-H7 ASSOCIATED WITH BLOODY DIARRHEA AND DEATH.* Annals of Internal Medicine, 1992. **117**(10): p. 812-819.

50. Macdonald, K.L., et al., *ESCHERICHIA-COLI O157-H7, AN EMERGING GASTROINTESTINAL PATHOGEN - RESULTS OF A ONE-YEAR, PROSPECTIVE, POPULATION-BASED STUDY.* Jama-Journal of the American Medical Association, 1988. **259**(24): p. 3567-3570.

51. Ostroff, S.M., J.M. Kobayashi, and J.H. Lewis, *INFECTIONS WITH ESCHERICHIA-COLI O157-H7 IN WASHINGTON STATE - THE 1ST YEAR OF STATEWIDE DISEASE SURVEILLANCE.* Jama-Journal of the American Medical Association, 1989. **262**(3): p. 355-359.

52. Pai, C.H., et al., *EPIDEMIOLOGY OF SPORADIC DIARRHEA DUE TO VEROCYTOTOXIN-PRODUCING ESCHERICHIA-COLI - A 2-YEAR PROSPECTIVE-STUDY.* Journal of Infectious Diseases, 1988. **157**(5): p. 1054-1057.

53. Pai, C.H., et al., *SPORADIC CASES OF HEMORRHAGIC COLITIS ASSOCIATED WITH ESCHERICHIA-COLI O157-H7 - CLINICAL, EPIDEMIOLOGIC, AND BACTERIOLOGIC FEATURES.* Annals of Internal Medicine, 1984. **101**(6): p. 738-742.

54. Ratnam, S. and S.B. March, *SPORADIC OCCURRENCE OF HEMORRHAGIC COLITIS ASSOCIATED WITH ESCHERICHIA-COLI O157-H7 IN NEWFOUNDLAND.* Canadian Medical Association Journal, 1986. **134**(1): p. 43-&.

55. Remis, R.S., et al., *SPORADIC CASES OF HEMORRHAGIC COLITIS ASSOCIATED WITH ESCHERICHIA-COLI O157-H7.* Annals of Internal Medicine, 1984. **101**(5): p. 624-626.

56. Cahoon, F.E. and J.S. Thompson, *FREQUENCY OF ESCHERICHIA-COLI O157-H7 ISOLATION FROM STOOL SPECIMENS.* Canadian Journal of Microbiology, 1987. **33**(10): p. 914-915.

57. Gransden, W.R., et al., *FURTHER EVIDENCE ASSOCIATING HEMOLYTIC UREMIC SYNDROME WITH INFECTION BY VEROTOXIN-PRODUCING ESCHERICHIA-COLI O157-H7.* Journal of Infectious Diseases, 1986. **154**(3): p. 522-524.

58. INNOCENT, G.T., et al., *Spatial and temporal epidemiology of sporadic human cases of Escherichia coli O157 in Scotland, 1996–1999.* Epidemiology & Infection, 2005. **133**(06): p. 1033-1041.

59. Waters, J.R., J.C. Sharp, and V.J. Dev, *Infection caused by Escherichia coli O157: H7 in Alberta, Canada, and in Scotland: a five-year review, 1987–1991.* Clinical infectious diseases, 1994. **19**(5): p. 834-843.

60. Griffin, P.M. and R.V. Tauxe, *The epidemiology of infections caused by Escherichia coli O157: H7, other enterohemorrhagic E. coli, and the associated hemolytic uremic syndrome.* Epidemiologic reviews, 1991. **13**(1): p. 60-98.

61. Lopez, E.L., et al., *Hemolytic uremic syndrome and diarrhea in Argentine children: the role of Shiga-like toxins.* Journal of Infectious Diseases, 1989. **160**(3): p. 469-475.

62. Rivas, M., et al., *Síndrome urémico hemolítico en niños de Mendoza, Argentina. Asociación con la infección por Escherichia coli productor de toxina shiga.* 1998.

63. MacDonald, I., I. Gould, and J. Curnow, *Epidemiology of infection due to Escherichia coli O157: a 3-year prospective study.* Epidemiology and infection, 1996. **116**(03): p. 279-284.

64. Pierard, D., *Infections with verotoxin-producing Escherichia coli.* Acta Clinica Belgica, 1991. **47**(6): p. 387-396.

65. Chapman, P., et al., *A 1-year study of Escherichia coli O157 in cattle, sheep, pigs and poultry.* Epidemiology and infection, 1997. **119**(02): p. 245-250.

66. Keene, W.E., et al., *An outbreak of Escherichia coli 0157: H7 infections traced to jerky made from deer meat.* Jama, 1997. **277**(15): p. 1229-1231.

67. ComoSabetti, K., et al., *Outbreaks of Escherichia coli O157: H7 infection associated with eating alfalfa sprouts-Michigan and Virginia, June-July 1997 (Reprinted from MMWR, vol 46, pg 741-744, 1997)*. 1997, AMER MEDICAL ASSOC 515 N STATE ST, CHICAGO, IL 60610. p. 809-810.

68. Akashi, S., et al., *A severe outbreak of haemorrhagic colitis and haemolytic uraemic syndrome*

associated withEscherichia coli 0157: H7 in Japan. European journal of pediatrics, 1994. **153**(9): p. 650-655.

69. Keene, W.E., et al., *A swimming-associated outbreak of hemorrhagic colitis caused by Escherichia coli O157: H7 and Shigella sonnei.* New England Journal of Medicine, 1994. **331**(9): p. 579-584.

70. Pavia, A.T., et al., *Hemolytic-uremic syndrome during an outbreak of< i> Escherichia coli</i> O157: H7 infections in institutions for mentally retarded persons: Clinical and epidemiologic observations.* The Journal of pediatrics, 1990. **116**(4): p. 544-551.

71. Swerdlow, D.L. and P.M. Griffin, *Duration of faecal shedding of< i> Escherichia coli</i> O157: H7 among children in day-care centres.* The Lancet, 1997. **349**(9054): p. 745-746.

72. Jo, B.-H., et al., *Three-dimensional micro-channel fabrication in polydimethylsiloxane (PDMS) elastomer.* Microelectromechanical Systems, Journal of, 2000. **9**(1): p. 76-81.

73. McDonald, J.C., et al., *Fabrication of microfluidic systems in poly(dimethylsiloxane).* ELECTROPHORESIS, 2000. **21**(1): p. 27-40.

74. Anderson, J.R., et al., *Fabrication of microfluidic systems in poly (dimethylsiloxane).* Electrophoresis, 2000. **21**: p. 27-40.

75. Levenson, M.D., N. Viswanathan, and R.A. Simpson, *Improving resolution in photolithography with a phase-shifting mask.* Electron Devices, IEEE Transactions on, 1982. **29**(12): p. 1828-1836.

76. Ashby, C.I., et al., *Formation of microchannels from low-temperature plasma-deposited silicon oxynitride*. 2000, Google Patents.

77. Rogers, J.A. and R.G. Nuzzo, *Recent progress in soft lithography.* Materials today, 2005. **8**(2): p. 50-56.

78. Hillborg, H., et al., *Crosslinked polydimethylsiloxane exposed to oxygen plasma studied by neutron reflectometry and other surface specific techniques.* Polymer, 2000. **41**(18): p. 6851-6863.

79. Bhattacharya, S., et al., *Studies on surface wettability of poly (dimethyl) siloxane (PDMS) and glass under oxygen-plasma treatment and correlation with bond strength.* Microelectromechanical Systems, Journal of, 2005. **14**(3): p. 590-597.

80. Goddard, J.M. and J. Hotchkiss, *Polymer surface modification for the attachment of bioactive compounds.* Progress in polymer science, 2007. **32**(7): p. 698-725.

81. Kingshott, P., H. Thissen, and H.J. Griesser, *Effects of cloud-point grafting, chain length, and density of PEG layers on competitive adsorption of ocular proteins.* Biomaterials, 2002. **23**(9): p. 2043-2056.

82. Lee, J.N., et al., *Compatibility of mammalian cells on surfaces of poly (dimethylsiloxane).* Langmuir, 2004. **20**(26): p. 11684-11691.

83. Wu, C.-C., C.-Y. Yuan, and S.-J. Ding, *Effect of polydimethylsiloxane surfaces silanized with different nitrogen-containing groups on the adhesion progress of epithelial cells.* Surface and Coatings Technology, 2011. **205**(10): p. 3182-3189.

84. Yeh, P.-Y., J.N. Kizhakkedathu, and M. Chiao, *A novel method to attenuate protein adsorption using combinations of polyethylene glycol (PEG) grafts and piezoelectric actuation.* Journal of Nanotechnology in Engineering and Medicine, 2010. **1**(4): p. 041010.

85. Zhang, Z., P. Zhao, and G. Xiao, *The fabrication of polymer microfluidic devices using a solid-to-solid interfacial polyaddition.* Polymer, 2009. **50**(23): p. 5358-5361.

86. Séguin, C., et al., *Surface modification of poly (dimethylsiloxane) for microfluidic assay applications.* Applied Surface Science, 2010. **256**(8): p. 2524-2531.

87. France, R., R. Short, and R. Dawson, *Attachment of human keratinocytes to plasma co-polymers of acrylic acid/octa-1, 7-diene and allyl amine/octa-1, 7-diene.* Journal of Materials Chemistry, 1998. **8**(1): p. 37-42.

88. Chowdhury, P.B. and P.F. Luckham, *Probing recognition process between an antibody and an antigen using atomic force microscopy.* Colloids and Surfaces A: Physicochemical and Engineering Aspects, 1998. **143**(1): p. 53-57.

89. Bernard, A., et al., *Affinity capture of proteins from solution and their dissociation by contact printing.* Nature biotechnology, 2001. **19**(9): p. 866-869.

90. Renault, J., et al., *Fabricating arrays of single protein molecules on glass using microcontact printing.* The Journal of Physical Chemistry B, 2003. **107**(3): p. 703-711.

91. Liu, D., et al., *Immobilization of DNA onto poly (dimethylsiloxane) surfaces and application to a microelectrochemical enzyme-amplified DNA hybridization assay.* Langmuir, 2004. **20**(14): p.

5905-5910.

92. Fixe, F., et al., *Electric-field-pulse-assisted covalent immobilization of DNA in the nanosecond time scale.* Applied physics letters, 2003. **83**(7): p. 1465-1467.

93. Arroyo-Hernandez, M., et al., *Biofunctionalization of surfaces of nanostructured porous silicon.* Materials Science and Engineering: C, 2003. **23**(6): p. 697-701.

94. Peramo, A., A. Albritton, and G. Matthews, *Deposition of patterned glycosaminoglycans on silanized glass surfaces.* Langmuir, 2006. **22**(7): p. 3228-3234.

95. Sierakowski, M.-R., et al., *Adsorption behavior of oxidized galactomannans onto amino-terminated surfaces and their interaction with bovine serum albumin.* Carbohydrate polymers, 2002. **49**(2): p. 167-175.

96. Vickers, J.A., M.M. Caulum, and C.S. Henry, *Generation of hydrophilic poly (dimethylsiloxane) for high-performance microchip electrophoresis.* Analytical Chemistry, 2006. **78**(21): p. 7446-7452.

97. Liu, Y., et al., *Dynamic coating using polyelectrolyte multilayers for chemical control of electroosmotic flow in capillary electrophoresis microchips.* Analytical chemistry, 2000. **72**(24): p. 5939-5944.

98. Ro, K.W., et al., *Capillary electrochromatography and preconcentration of neutral compounds on poly (dimethylsiloxane) microchips.* Electrophoresis, 2003. **24**(18): p. 3253-3259.

99. Xiao, D., H. Zhang, and M. Wirth, *Chemical modification of the surface of poly (dimethylsiloxane) by atom-transfer radical polymerization of acrylamide.* Langmuir, 2002. **18**(25): p. 9971-9976.

100. Kim, S.H., et al., *Simple Route to Hydrophilic Microfluidic Chip Fabrication Using an Ultraviolet (UV)-Cured Polymer.* Advanced Functional Materials, 2007. **17**(17): p. 3493-3498.

101. Wu, T., K. Efimenko, and J. Genzer, *Combinatorial study of the mushroom-to-brush crossover in surface anchored polyacrylamide.* Journal of the american chemical society, 2002. **124**(32): p. 9394-9395.

102. Tugulu, S. and H.A. Klok. *Surface modification of polydimethylsiloxane substrates with nonfouling poly (poly (ethylene glycol) methacrylate) brushes*. in *Macromolecular symposia*. 2009. Wiley Online Library.

103. Sasaki, H., et al., *Parylene-coating in PDMS microfluidic channels prevents the absorption of fluorescent dyes.* Sensors and Actuators B: Chemical, 2010. **150**(1): p. 478-482.

104. Zhang, Z., et al., *"Click" chemistry-based surface modification of poly (dimethylsiloxane) for protein separation in a microfluidic chip.* Electrophoresis, 2010. **31**(18): p. 3129-3136.

105. Zhang, Z., et al., *Environmentally friendly surface modification of PDMS using PEG polymer brush.* Electrophoresis, 2009. **30**(18): p. 3174-3180.

106. Tomalia, D.A., et al., *A new class of polymers: starburst-dendritic macromolecules.* Polymer Journal, 1985. **17**(1): p. 117-132.

107. Bieniarz, C., *Dendrimers: applications to pharmaceutical and medicinal chemistry.* Encyclopedia of pharmaceutical technology, 1998. **18**(Suppl 1): p. 55-89.

108. Tomalia, D.A., A.M. Naylor, and W.A. Goddard, *Starburst dendrimers: molecular-level control of size, shape, surface chemistry, topology, and flexibility from atoms to macroscopic matter.* Angewandte Chemie International Edition in English, 1990. **29**(2): p. 138-175.

109. Tomalia, D. and P. Dvornic, *Dendritic polymers, divergent synthesis (Starburst polyamidoamine dendrimers).* Polymeric materials encyclopedia, 1996. **3**: p. 1814-1830.

110. Hawker, C.J. and J.M. Frechet, *Preparation of polymers with controlled molecular architecture. A new convergent approach to dendritic macromolecules.* Journal of the American Chemical Society, 1990. **112**(21): p. 7638-7647.

111. Newkome, G., C. Moorefield, and F. Vögtle, *Synthetic methodologies: convergent procedures.* Dendritic Molecules: Concepts, Syntheses, Perspectives, 1996: p. 107-163.

112. Wooley, K.L., C.J. Hawker, and J.M. Fréchet, *Polymers with controlled molecular architecture: control of surface functionality in the synthesis of dendritic hyperbranched macromolecules using the convergent approach.* Journal of the Chemical Society, Perkin Transactions 1, 1991(5): p. 1059-1076.

113. Tomalia, D., et al. *Dendritic macromolecules: a fourth major class of polymer architecture–new properties driven by architecture*. in *MRS Proceedings*. 1998. Cambridge Univ Press.

114. Eichman, J.D., et al., *The use of PAMAM dendrimers in the efficient transfer of genetic material into cells.* Pharmaceutical science & technology today, 2000. **3**(7): p. 232-245.

115. Lothian-Tomalia, M.K., et al., *A contemporary survey of covalent connectivity and complexity.*

The divergent synthesis of poly (thioether) dendrimers. Amplified, genealogically directed synthesis leading to the de Gennes dense packed state. Tetrahedron, 1997. **53**(45): p. 15495-15513.

116. Pötschke, D., et al., *Analysis of the structure of dendrimers in solution by small-angle neutron scattering including contrast variation.* Macromolecules, 1999. **32**(12): p. 4079-4087.

117. Liu, M. and J.M. Fréchet, *Designing dendrimers for drug delivery.* Pharmaceutical Science & Technology Today, 1999. **2**(10): p. 393-401.

118. Tomalia, D.A., M. Hall, and D.M. Hedstrand, *Starburst dendrimers. III. The importance of branch junction symmetry in the development of topological shell molecules.* Journal of the American Chemical Society, 1987. **109**(5): p. 1601-1603.

119. Ottaviani, M.F., et al., *Characterization of starburst dendrimers by the EPR technique. Copper (II) ions binding full-generation dendrimers.* The Journal of Physical Chemistry B, 1997. **101**(2): p. 158-166.

120. Pesak, D.J., J.S. Moore, and T.E. Wheat, *Synthesis and characterization of water-soluble dendritic macromolecules with a stiff, hydrocarbon interior.* Macromolecules, 1997. **30**(21): p. 6467-6482.

121. Schwartz, B.L., et al., *Detection of high molecular weight starburst dendrimers by electrospray ionization mass spectometry.* Rapid communications in mass spectrometry, 1995. **9**(15): p. 1552-1555.

122. Wiener, E., et al., *Dendrimer-based metal chelates: A new class of magnetic resonance imaging contrast agents.* Magnetic resonance in medicine, 1994. **31**(1): p. 1-8.

123. Evenson, S.A. and J.P.S. Badyal, *Self-assembled PAMAM dendrimer films.* Advanced Materials, 1997. **9**(14): p. 1097-1099.

124. Li, J., et al., *Visualization and characterization of poly (amidoamine) dendrimers by atomic force microscopy.* Langmuir, 2000. **16**(13): p. 5613-5616.

125. Saville, P., et al., *Dendrimer and polystyrene surfactant structure at the air-water interface.* The Journal of Physical Chemistry, 1993. **97**(2): p. 293-294.

126. Shi, X., et al., *Analysis of poly (amidoamine)-succinamic acid dendrimers by slab-gel electrophoresis and capillary zone electrophoresis.* Electrophoresis, 2005. **26**(15): p.

2960-2967.

127. Uppuluri, S., et al., *Core–shell tecto (dendrimers): I. Synthesis and characterization of saturated shell models.* Advanced Materials, 2000. **12**(11): p. 796-800.

128. Selkoe, D.J., *Folding proteins in fatal ways.* Nature, 2003. **426**(6968): p. 900-904.

129. Kitchens, K.M., M.E. El-Sayed, and H. Ghandehari, *Transepithelial and endothelial transport of poly (amidoamine) dendrimers.* Advanced drug delivery reviews, 2005. **57**(15): p. 2163-2176.

130. Caminade, A.M., C.O. Turrin, and J.P. Majoral, *Dendrimers and DNA: combinations of two special topologies for nanomaterials and biology.* Chemistry-a European Journal, 2008. **14**(25): p. 7422-7432.

131. Jevprasesphant, R., et al., *Transport of dendrimer nanocarriers through epithelial cells via the transcellular route.* Journal of controlled release, 2004. **97**(2): p. 259-267.

132. Paleos, C.M., et al., *Gene delivery using functional dendritic polymers.* 2009.

133. Gao, Y., et al., *Recent advances of dendrimers in delivery of genes and drugs.* Mini reviews in medicinal chemistry, 2008. **8**(9): p. 889-900.

134. Hong, B.J., et al., *Nanoscale-controlled spacing provides DNA microarrays with the SNP discrimination efficiency in solution phase.* Langmuir, 2005. **21**(10): p. 4257-4261.

135. Jung, Y.J., et al., *Dendron arrays for the force-based detection of DNA hybridization events.* Journal of the American Chemical Society, 2007. **129**(30): p. 9349-9355.

136. Benters, R., C. Niemeyer, and D. Wöhrle, *Dendrimer-activated solid supports for nucleic acid and protein microarrays.* ChemBioChem, 2001. **2**(9): p. 686-694.

137. Chaize, B., et al., *Microstructured liposome array.* Bioconjugate chemistry, 2006. **17**(1): p. 245-247.

138. Lim, S.B., et al., *Improved DNA chip with poly (amidoamine) dendrimer peripherally modified with biotin and avidin.* Biotechnology and Bioprocess Engineering, 2008. **13**(6): p. 683-689.

139. Bhatnagar, P., et al., *Dendrimer-Scaffold-Based Electron-Beam Patterning of Biomolecules.* Advanced Materials, 2006. **18**(3): p. 315-319.

140. Yalow, R.S. and S.A. Berson, *Assay of plasma insulin in human subjects by immunological methods.* 1959.

141. Köhler, G. and C. Milstein, *Continuous cultures of fused cells secreting antibody of predefined*

specificity. Nature, 1975. **256**(5517): p. 495-497.

142. Hybarger, G., et al., *A microfluidic SELEX prototype.* Analytical and bioanalytical chemistry, 2006. **384**(1): p. 191-198.

143. Lou, X., et al., *Micromagnetic selection of aptamers in microfluidic channels.* Proceedings of the National Academy of Sciences, 2009. **106**(9): p. 2989-2994.

144. Kirby, R., et al., *Aptamer-based sensor arrays for the detection and quantitation of proteins.* Analytical Chemistry, 2004. **76**(14): p. 4066-4075.

145. Mosing, R.K. and M.T. Bowser, *Microfluidic selection and applications of aptamers.* Journal of separation science, 2007. **30**(10): p. 1420-1426.

146. Situma, C., M. Hashimoto, and S.A. Soper, *Merging microfluidics with microarray-based bioassays.* Biomolecular engineering, 2006. **23**(5): p. 213-231.

147. Mairhofer, J., K. Roppert, and P. Ertl, *Microfluidic systems for pathogen sensing: a review.* Sensors, 2009. **9**(6): p. 4804-4823.

148. Bouvrette, P. and J. Luong, *Development of a flow injection analysis (FIA) immunosensor for the detection of< i> Escherichia coli</i>.* International journal of food microbiology, 1995. **27**(2): p. 129-137.

149. Yu, H. and J.G. Bruno, *Immunomagnetic-electrochemiluminescent detection of Escherichia coli O157 and Salmonella typhimurium in foods and environmental water samples.* Applied and environmental microbiology, 1996. **62**(2): p. 587-592.

150. Vernozy-Rozand, C., et al., *Detection of Escherichia coli O157 in French food samples using an immunomagnetic separation method and the VIDASTME. coli O157.* Letters in applied microbiology, 1997. **25**(6): p. 442-446.

151. Brewster, J.D. and R.S. Mazenko, *Filtration capture and immunoelectrochemical detection for rapid assay of Escherichia coli O157: H71.* Journal of Immunological methods, 1998. **211**(1-2): p. 1-8.

152. Pérez, F.G., et al., *Immunomagnetic separation with mediated flow injection analysis amperometric detection of viable Escherichia coli O157.* Analytical chemistry, 1998. **70**(11): p. 2380-2386.

153. Abdel-Hamid, I., et al., *Flow-through immunofiltration assay system for rapid detection of< i>*

E</i>.< i> coli</i> O157: H7. Biosensors and Bioelectronics, 1999. **14**(3): p. 309-316.

154. Liu, G., et al., *Aptamer– Nanoparticle Strip Biosensor for Sensitive Detection of Cancer Cells.* Analytical chemistry, 2009. **81**(24): p. 10013-10018.

155. Dharmasiri, U., et al., *Highly efficient capture and enumeration of low abundance prostate cancer cells using prostate-specific membrane antigen aptamers immobilized to a polymeric microfluidic device.* Electrophoresis, 2009. **30**(18): p. 3289-3300.

156. Huang, P.-J.J. and J. Liu, *Flow cytometry-assisted detection of adenosine in serum with an immobilized aptamer sensor.* Analytical chemistry, 2010. **82**(10): p. 4020-4026.

157. Soontornworajit, B. and Y. Wang, *Nucleic acid aptamers for clinical diagnosis: cell detection and molecular imaging.* Analytical and bioanalytical chemistry, 2011. **399**(4): p. 1591-1599.

158. Obubuafo, A., et al., *Poly (methyl methacrylate) microchip affinity capillary gel electrophoresis of aptamer–protein complexes for the analysis of thrombin in plasma.* Electrophoresis, 2008. **29**(16): p. 3436-3445.

159. Gong, M., et al., *Detection of VEGF165 Using an Aptamer Affinity Probe in Microchip Capillary Electrophoresis.* Current Pharmaceutical Analysis, 2009. **5**(2): p. 156-163.

160. Lin, M.-C., et al., *Rapid detection of natriuretic peptides by a microfluidic LabChip analyzer with DNA aptamers: Application of natriuretic peptide detection.* Biomicrofluidics, 2009. **3**(3): p. 034101.

161. Cho, S., et al., *Microbead-based affinity chromatography chip using RNA aptamer modified with photocleavable linker.* Electrophoresis, 2004. **25**(21-22): p. 3730-3739.

162. Chung, W.J., et al., *Microaffinity purification of proteins based on photolytic elution: toward an efficient microbead affinity chromatography on a chip.* Electrophoresis, 2005. **26**(3): p. 694-702.

163. Yang, Y.-N., et al., *An integrated microfluidic system for C-reactive protein measurement.* Biosensors and Bioelectronics, 2009. **24**(10): p. 3091-3096.

164. Schlensog, M.D., et al., *A Love-wave biosensor using nucleic acids as ligands.* Sensors and Actuators B: Chemical, 2004. **101**(3): p. 308-315.

165. Jung, A., et al., *Biofunctional structural design of SAW sensor chip surfaces in a microfluidic sensor system.* Sensors and Actuators B: Chemical, 2007. **124**(1): p. 46-52.

166. Phillips, J.A., et al., *Enrichment of cancer cells using aptamers immobilized on a microfluidic channel.* Analytical chemistry, 2008. **81**(3): p. 1033-1039.

167. Ho, D., et al., *DNA as a force sensor in an aptamer-based biochip for adenosine.* Analytical chemistry, 2009. **81**(8): p. 3159-3164.

168. Tennico, Y.H., et al., *On-chip aptamer-based sandwich assay for thrombin detection employing magnetic beads and quantum dots.* Analytical chemistry, 2010. **82**(13): p. 5591-5597.

169. Wang, H., et al., *Microfluidic chip-based aptasensor for amplified electrochemical detection of human thrombin.* Electrochemistry Communications, 2010. **12**(2): p. 258-261.

170. Nguyen, T.H., et al., *An aptameric microfluidic system for specific purification, enrichment, and mass spectrometric detection of biomolecules.* Microelectromechanical Systems, Journal of, 2009. **18**(6): p. 1198-1207.

171. Nguyen, T., et al., *An aptamer-based microfluidic device for thermally controlled affinity extraction.* Microfluidics and nanofluidics, 2009. **6**(4): p. 479-487.

172. Nguyen, T., et al., *Microfluidic aptameric affinity sensing of vasopressin for clinical diagnostic and therapeutic applications.* Sensors and Actuators B: Chemical, 2011. **154**(1): p. 59-66.

173. Uppuluri, S., et al., *Core–shell tecto (dendrimers): I. Synthesis and characterization of saturated shell models.* Advanced Materials, 2000. **12**(11): p. 796-800.

174. Wu, W., et al., *An aptamer-based biosensor for colorimetric detection of Escherichia coli O157: H7.* PloS one, 2012. **7**(11): p. e48999.

175. Qin, Y., et al., *Developing an ultra non-fouling SU-8 and PDMS hybrid microfluidic device by poly (amidoamine) engraftment.* Colloids and Surfaces B: Biointerfaces, 2015. **127**: p. 247-255.

176. Holländer, A., *Labelling techniques for the chemical analysis of polymer surfaces.* Surface and interface analysis, 2004. **36**(8): p. 1023-1026.

177. Siow, K.S., et al., *Plasma Methods for the Generation of Chemically Reactive Surfaces for Biomolecule Immobilization and Cell Colonization-A Review.* Plasma Processes and Polymers, 2006. **3**(6-7): p. 392-418.

178. Scrimgeour, J., et al., *Photobleaching-activated micropatterning on self-assembled monolayers.* Journal of Physics: Condensed Matter, 2010. **22**(19): p. 194103.

179. Mu, C., et al., *Development of a simple and reliable PDMS interconnect for high throughput*

microfluidic applications. Microsystem Technologies, 2013. **21**(1): p. 147-154.

180. Du, Y., et al., *A simplified design of the staggered herringbone micromixer for practical applications.* Biomicrofluidics, 2010. **4**(2): p. 024105.

181. Goddard, J.M. and D. Erickson, *Bioconjugation techniques for microfluidic biosensors.* Analytical and bioanalytical chemistry, 2009. **394**(2): p. 469-479.

182. Biajoli, A.F. and F. Augusto, *Solid phase microextraction fibers coated with sol-gel aminopropylsilica/polydimethylsiloxane: Development and its application to screening of beer headspace.* Analytical Sciences, 2008. **24**(9): p. 1141.

183. Allauddin, S., et al., *Synthesis and characterization of APTMS/melamine cured hyperbranched polyester-epoxy hybrid coatings.* Progress in Organic Coatings, 2013. **76**(10): p. 1402-1412.

184. Jung, H.-S., D.-S. Moon, and J.-K. Lee, *Quantitative analysis and efficient surface modification of silica nanoparticles.* Journal of Nanomaterials, 2012. **2012**: p. 48.

185. Fritz, J.L. and M.J. Owen, *Hydrophobic recovery of plasma-treated polydimethylsiloxane.* The Journal of Adhesion, 1995. **54**(1-4): p. 33-45.

186. Lawton, R.A., et al., *Air plasma treatment of submicron thick PDMS polymer films: effect of oxidation time and storage conditions.* Colloids and Surfaces A: Physicochemical and Engineering Aspects, 2005. **253**(1): p. 213-215.

187. Briand, E., et al., *Chemical Modifications of Au/SiO2 Template Substrates for Patterned Biofunctional Surfaces.* Langmuir, 2010. **27**(2): p. 678-685.

188. Xu, Z.X., et al., *Amide-linkage formed between ammonia plasma treated poly (D, L-lactide acid) scaffolds and bio-peptides: Enhancement of cell adhesion and osteogenic differentiation in vitro.* Biopolymers, 2011. **95**(10): p. 682-694.

189. Crist, B.V., *Handbook of monochromatic XPS spectra, The elements of native Oxides.* Handbook of Monochromatic XPS Spectra, The Elements of Native Oxides, by B. Vincent Crist, pp. 548. ISBN 0-471-49265-5. Wiley-VCH, October 2000., 2000. **1**.

190. Walther, F., et al., *Stability of the hydrophilic behavior of oxygen plasma activated SU-8.* Journal of Micromechanics and Microengineering, 2007. **17**(3): p. 524.

191. Zhao, X., et al., *Engineering amphiphilic membrane surfaces based on PEO and PDMS segments for improved antifouling performances.* Journal of Membrane Science, 2014. **450**: p. 111-123.

192. Yeh, P.-Y.J., et al., *Self-assembled monothiol-terminated hyperbranched polyglycerols on a gold surface: a comparative study on the structure, morphology, and protein adsorption characteristics with linear poly (ethylene glycol) s.* Langmuir, 2008. **24**(9): p. 4907-4916.

193. Stroock, A.D., et al., *Chaotic mixer for microchannels.* Science, 2002. **295**(5555): p. 647-651.

Appendices

A1. PAMAM Modification Protocols

1. Protocol of carboxyl modified PAMAM: PAMAM (0.3g) with the addition of succinic anhydride (0.02g) for 4h at room temperature in 2 ml PBS (pH 7.4). Then dialysis the former solution in DI water for 2 days dialysis tube. (Slide-A-Lyzer Dialysis Cassette, 10k MWCO, Thermo Scientific) 2. Carboxyl modify PAMAM with rhodamine: PAMAM (0.3g) with 0.1ml former prepared NHS-rhodamine (NHS-rhodamine dissolved in DMF at 10mg/ml) and succinic anhydride (0.02g) for 4h at room temperature in 2 ml PBS (pH 7.4).Then dialysis the former solution in DI water for 2 days using dialysis tube.(Slide-A-Lyzer Dialysis Cassette, 10k MWCO, Thermo Scientific)

A2. Figure of PAMAM Conjugation Conditions Tests